

Ac

KUNS 1335  
April 11, 1995

CERN LIBRARIES, GENEVA



SCAN-9507222

SW 9530

I. INTRODUCTION

## Central Force of the Hyperon-Nucleon Interaction in the $SU_6$ Quark Model

Choki NAKAMOTO, Yasuyuki SUZUKI\* and Yoshikazu FUJIWARA\*\*

Graduate School of Science and Technology, Niigata University, Niigata 950-21

\*Department of Physics, Niigata University, Niigata 950-21

\*\*Department of Physics, Kyoto University, Kyoto 606-01

### Abstract

Characteristic properties of the medium-range central attraction of the nucleon-nucleon and hyperon-nucleon interactions are studied in the  $(3q)-(3q)$  resonating-group formulation. The  $SU_6$  properties of two-baryon systems are extensively incorporated with the explicit flavor symmetry breaking of the full Fermi-Breit residual interaction. It is found that, for a realistic quark-model description of the hyperon-nucleon interaction compatible with the present low-energy experimental data, it is necessary to introduce phenomenological medium-range attraction which is much less than that for the nucleon-nucleon system. Effective meson-exchange potentials from the scalar-meson nonet exchange in the Nijmegen model-F are conveniently employed to generate the needed flavor-dependent central attraction with few parameters determined for each flavor exchange symmetry.

The study of the hyperon-nucleon ( $YN$ ) interaction has basic importance not only for applications to hypernuclear physics,<sup>1)</sup> but also for elucidating rich phenomena of the strong interaction dominated by the quark-gluon dynamics through QCD. In contrast with the nucleon-nucleon ( $NN$ ) interaction, direct experimental analysis of elementary  $YN$  scattering processes is not possible at present, resulting in very scarce experimental information of low-energy cross-section data with large error bars. From the theoretical side, quite successful meson-exchange description of the  $NN$  interaction has been extended to the  $YN$  interaction recently, and several versions of the one boson exchange potentials (OBEP), such as the Nijmegen models<sup>2),3)</sup> and the Jülich potentials,<sup>4),5)</sup> are already available. As a common feature of these models, a large number of baryon-meson coupling constants are constrained by the use of the  $SU_3$  relations, in which several  $SU_3$  parameters are determined in the  $NN$  sector, supplemented with the low-energy cross-section data for the  $YN$  scattering. Since the short-range repulsion, well established in the  $NN$  interaction, is now believed to have its origin in the quark-gluon dynamics, the treatment of this short-range part in the above OBEP's is more or less phenomenological.

The most successful quark-model study of the baryon-baryon interaction is carried out in the resonating-group method (RGM) applied to the  $(3q)-(3q)$  system, in which the gluon effect is incorporated through the color analog of the Fermi-Breit interaction in the one-gluon exchange approximation and a simple power-law confinement potential put in by hand. The conclusion of such calculations for the  $NN$  interaction<sup>6)</sup> can be summarized as follows: The phase-shift equivalent effective local potentials derived from the  $(3q)-(3q)$  models of  $NN$  scattering are short-ranged, strongly energy dependent and purely repulsive. The repulsive core of several hundred MeV is determined largely by the color-magnetic term of the Fermi-Breit interaction. The coupling to other channels of the  $(3q)-(3q)$  variety such as the  $\Delta$ - $\Delta$  and the so-called hidden color channels has been found not to play a prominent role, but only leads to small refinements. Since the simple  $(3q)-(3q)$  RGM cannot

account for the medium- and long-range attraction of the  $NN$  interaction, effective meson-exchange potentials are usually introduced to achieve a realistic description of the  $NN$  interaction. In the recent quark-model analysis of the  $NN$  interaction by Takeuchi et al.,<sup>7)</sup> the central attraction originating from scalar-meson exchange potentials is introduced for each of the  $^1E$ ,  $^3E$ ,  $^1O$  and  $^3O$  states, as well as the spin-spin and the tensor forces of the one-pion exchange potential. Another attempt to incorporate the meson-exchange effects is the explicit introduction of  $(q\bar{q})$  and  $(q\bar{q})^2$  excitations. Without introducing any extra meson parameters, this extended quark model<sup>8)</sup> was quite successful in reproducing the main features of the  $NN$  interaction, leading to the first step toward the conventional meson-exchange description through the possible mechanism of  $(q\bar{q})$  exchanges between nucleons.

The extension of the  $(3q)$ - $(3q)$  RGM study of the  $NN$  interaction to the  $YN$  interaction is not trivial particularly with respect to the central force. The reason is the following: 1) The lack of the medium-range attraction in the quark model leads to too much ambiguity in the way of supplementing the effective meson-exchange potentials. 2) In the  $YN$  interaction, the flavor-symmetry breaking (FSB) should be naturally introduced even though we choose the spin-flavor  $SU_6$  symmetry as the starting point. For example, Oka, Shimizu and Yazaki<sup>9)</sup> have studied only the short-range repulsion originating from the color-magnetic piece and discussed the correlation of the repulsion with the eigen-values of the  $(3q)$ - $(3q)$  normalization kernel for octet- and decuplet-baryon systems. The work by Straub et al.<sup>10)</sup> has dealt with the low-energy cross sections by incorporating effective meson-exchange potentials. Unfortunately, their fit to the experimental data is obtained by a large number of phenomenological parameters introduced both in the quark sector and in the effective meson-exchange sector, and gives little information about characters of effective meson-exchange potentials put in by hand. We believe that this is caused by the way they treat the FSB in the quark sector. The paper by Zhang et al.<sup>11)</sup> is an attempt to find a set of common meson-exchange parameters for the  $NN$  and  $YN$  systems by employing meson-exchange potentials constrained by the chiral symmetry requirement.

Our viewpoint for applying the RGM formalism to the  $YN$  interaction is based on the

premise that the  $SU_6$  quark model with some realistic modification like peripheral mesonic or  $(q\bar{q})$  effects can essentially reproduce the whole low-energy hadronic phenomena. As long as the low-energy observables are concerned, predictions of the Fermi-Breit interaction have no obvious disagreement with experiment except for the  $\pi$  and  $\eta'$  properties and the so-called "missing  $LS$  force problem" of  $P$ -wave baryons. The extremely small mass of the pion is due to its Goldstone-boson aspect associated with the spontaneous breaking of the chiral symmetry at the quark level, and the abnormally large mass of  $\eta'$  is related to the typical multi-gluon effect called  $U_A(1)$  anomaly. In the recent work<sup>12)</sup> by one of the present authors, it is found that a long-standing problem of the missing  $LS$  force of the Fermi-Breit interaction in the excited states of baryons can possibly be resolved by a proper treatment of a compact  $(3q)$  structure embedded in the  $(3q)(q\bar{q})$  continua. In a separate paper,<sup>13)</sup> we have shown that the same Fermi-Breit  $LS$  force has almost right order of magnitude compatible with the experimental information on the  $YN$  spin-orbit interaction. It is important to note that these conclusions are obtained by keeping the Galilean non-invariant terms contained in the Fermi-Breit interaction. Since the momentum-dependence involved in these terms can be properly treated in the RGM framework, we should not throw these terms away simply because they do not fit the non-relativistic framework.

In this paper we discuss characteristics of the medium-range attraction required in the overall description of the  $NN$  and  $YN$  interactions in terms of the  $(3q)$ - $(3q)$  RGM. Since our purpose is to study the missing part in the quark model, it is essential to deal with the quark sector very carefully and to minimize the theoretical ambiguity related to the pure quark-model potentials. This can be achieved by making the most of the spin-flavor  $SU_6$  symmetries of the octet-baryon ( $B_8$ ) systems, as well as by correct treatment of the FSB. Two- $B_8$  systems are classified in terms of the flavor symmetry with respect to the interchange of the two baryons, by which the discussion of the FSB becomes very transparent owing to the generalized Pauli principle. The FSB due to the mass difference between the strange and up-down quarks is explicitly introduced in the nonrelativistic kinetic-energy term and the residual Fermi-Breit interaction without any approximation. The spin-flavor factors of the

quark exchange kernels are analytically evaluated by using an extended operator formalism, which is particularly developed for this application.

It should be noted that we choose a rather simple model space for the two- $B_8$  system with respect to the spatial and spin-flavor degrees of freedom. The spatial extension of the quark distribution in each baryon is controlled by a common harmonic-oscillator constant  $b$ , which is supposed not to be much different among members of each  $SU_6$  supermultiplet. To scale  $b$  by the strange quark mass is sometimes used in the literature,<sup>10)</sup> but such a prescription causes a serious problem that an uncontrollable FSB ensues from the confinement potential which is originally assumed to be flavor independent. Instead, we take a perturbative viewpoint by using the pure  $SU_6$ -model wave functions, though we introduce the explicit FSB in the quark-model Hamiltonian.

We should keep in mind that application of the RGM formalism to the  $(3q)$ - $(3q)$  system is not actually straightforward, since the system we are dealing with is essentially relativistic. The standard non-relativistic RGM formulation should be augmented with some new features which are best tailored to the phenomena under consideration and are guided by the physical intuitions.<sup>14)</sup> For example, the separation of the center-of-mass (c.m.) motion is no longer a simple task when relativistic corrections are introduced into the kinetic-energy operators and/or the momentum-dependent retardation terms are taken into account. The non-relativistic definition of the c.m. coordinate for the systems involving unequal quark masses is not the best choice in this situation, since the inertia mass for the system is not simply given by the sum of the constituent quark masses. What we have to do is to go back to the original definition of the relative motion and consider the realistic situation of the scattering that two  $(3q)$  clusters are colliding with the incident momentum  $\mathbf{k}$  and  $-\mathbf{k}$ . Here we also come across the problem that the inertia mass of the  $(3q)$  system is not properly reproduced in any kind of the quark models, even if we succeed in fitting the energy splitting of the octet baryons. The reduced mass employed in the RGM equation should be, therefore, readjusted to the experimental value in some way, in order to ensure the correct scattering kinematics. We will present in this paper a nice prescription to do this without breaking

the Pauli principle.

A similar situation also takes place when we supplement the meson-exchange effect to the  $(3q)$ - $(3q)$  RGM. The meson-exchange effect is essentially a relativistic phenomenon related to the creation and annihilation processes of the  $(q\bar{q})$  pairs. Although the  $(q\bar{q})$  description of the meson-exchange effect in the  $YN$  interaction is attempted in Ref. 15), it is still restricted to the simple  $(q\bar{q})$  exchange processes, where correspondence to the meson-exchange potentials is best seen. The exchange kernels generated from more complicated quark-exchange diagrams are not fully analysed even at the phenomenological level. We will, therefore, adopt in this paper an intermediate step to introduce the effective meson-exchange potentials as employed by several authors.<sup>6),7),10)</sup> There are still many possibilities of how to generate these effective meson-exchange potentials. The simplest method is to use an effective local potential,  $V^{eff}$ , at the baryon level, which is determined from the existing OBEP's or in a rather arbitrary way to fit the experimental data. Since the correspondence between the RGM formalism for composite particles and the ordinary Schrödinger equation for structureless particles implies the renormalization of the relative-motion function multiplied by  $\sqrt{N}$  factor, with  $N$  being the normalization kernel, the nonlocal kernel of the form  $\sqrt{N}V^{eff}\sqrt{N}$  is usually introduced in the RGM equation. A nice point of this prescription is that we only need the normalization kernel to generate the exchange terms.

In order to make the analysis of the medium-range attraction of the  $YN$  interaction as transparent as possible, we will apply in this paper the semi-classical Wigner-transform WKB technique<sup>16)</sup> to the RGM equation. In this technique, the necessary momentum-dependent Wigner-transforms are analytically derived from the explicit expressions of the RGM kernels,<sup>17)</sup> and the phase-shift equivalent local potentials are easily obtained by solving a self-consistent transcendental equation which determines a local momentum for the relative motion. In particular, the effective nonlocal potential,  $\sqrt{N}V^{eff}\sqrt{N}$ , is simply reduced to the algebraic multiplication of  $V^{eff}$  and the Wigner transform of the normalization kernel within this approximation.

The organization of this paper is as follows. In the next section we first discuss some

properties of the spin-flavor symmetry of  $B_8$ - $B_8$  systems, which are shared by both quark model and OBEP's. The isospin basis with definite flavor symmetry introduced in this section facilitates a convenient scheme for state-classification of the  $YN$  system in a similar way to the  $NN$  system. The phase shift behavior of empirical OBEP's is discussed in conjunction with the  $SU_3$  content of the  $YN$  system with respect to the central part of the potentials. A brief formulation of the model is given in Section 3, by paying a special attention to the Galilean non-invariant term of the Fermi-Breit interaction, as well as the reduced mass of the kinetic-energy term. In Section 4, we examine the effect of the Pauli principle in a simple model in which the exchange kernels of the kinetic-energy and momentum-dependent terms are retained. We find that characteristic features of the central phase shifts for all the  $NN$ ,  $\Lambda N$  and  $\Sigma N$  channels are already understandable in this simple model. A realistic analysis with all the quark-model potentials and the effective meson-exchange potentials is carried out in Section 5. It is found that the central attraction which leads to the empirical phase-shift behavior of the  $\Lambda N$  and  $\Sigma N$  potentials inevitably needs to be smaller than that for the  $NN$  system. The last section is devoted to a brief summary and future directions.

## II. SPIN-FLAVOR SYMMETRIES OF $B_8$ - $B_8$ SYSTEMS

As a system of two unidentical particles, the  $YN$  interaction has several new features which are not shared with the  $NN$  interaction. These are mainly related to the rich flavor contents of the  $B_8$ - $B_8$  system constrained by the spin-flavor  $SU_6$  symmetry and the generalized Pauli principle. Since these features are common in both OBEP and quark-model, we will use baryon's degree of freedom as long as possible.

Let us use the Elliott notation to specify the  $SU_3$  quantum numbers of  $B_8$ , and let  $B_{(11)a}$  with  $a \equiv YI$  denote a flavor function  $N$  ( $YI = 1\frac{1}{2}$ ),  $\Lambda$  ( $YI = 00$ ),  $\Sigma$  ( $YI = 01$ ) or  $\Xi$  ( $YI = -1\frac{1}{2}$ ). The  $SU_3$ -coupled basis of two octet baryons is defined by

$$[B_{(11)}B_{(11)}]_{(\lambda\mu)\alpha;\rho} = [B_{(11)}(1)B_{(11)}(2)]_{(\lambda\mu)\alpha;\rho}$$

$$= \sum_{a_1, a_2} \langle (11)a_1(11)a_2 \parallel (\lambda\mu)a \rangle_{\rho} [B_{(11)a_1}(1)B_{(11)a_2}(2)]_{II_i}, \quad (2.1)$$

where the last square brackets denote the isospin coupling. We assume that the first  $B_{(11)}$  always refers to particle 1 and the second to particle 2. A set of the internal quantum numbers,  $\alpha$  ( $\alpha = aI_z$ ), stand for the hypercharge  $Y = Y_1 + Y_2$ , the total isospin  $I$  and its  $z$ -component  $I_z$ , which are all conserved quantities if we assume the isospin symmetry and the charge conservation  $Q/e = Y/2 + I_z$ . The flavor symmetry phase  $\mathcal{P}$  of the two-baryon system is defined by the flavor exchange operator  $P_{12}^F$  and is determined from the symmetry of the  $SU_3$  Clebsch-Gordan coefficients through

$$P_{12}^F [B_{(11)}B_{(11)}]_{(\lambda\mu)\alpha;\rho} = \mathcal{P} [B_{(11)}B_{(11)}]_{(\lambda\mu)\alpha;\rho}, \quad (2.2)$$

with

$$\mathcal{P} = \begin{cases} (-1)^{\lambda+\mu} & \text{in multiplicity-free case with } (\lambda\mu) \neq (11) \\ \pm 1 & \text{for } (\lambda\mu)_{\rho} = (11)_{(4)} \end{cases}. \quad (2.3)$$

It is important to maintain the definite flavor symmetry even in the isospin-coupled basis, since the flavor symmetry is related to the total spin  $S$  and the parity through the generalized Pauli principle;

$$(-1)^{L+S}\mathcal{P} = 1, \quad (2.4)$$

where  $L$  is the relative orbital angular momentum. For the  $NN$  system with  $Y = 2$ , the total isospin  $I$  is good enough to specify  $\mathcal{P}$ ; i.e.,  $\mathcal{P} = (-1)^{1-I}$ , so that Eq. (2.4) becomes the well-known rule  $(-1)^{L+S+I} = -1$ . Let us introduce a simplified notation  $B_i \equiv B_{(11)a_i}$  ( $i = 1 \sim 4$  in general) with  $a_i = Y_i I_i$ . The isospin basis used in this paper is the one with the definite flavor symmetry  $\mathcal{P}$ , and is defined through

$$\begin{aligned} [B_1 B_2]_{II_i}^{\mathcal{P}} &= \frac{1}{\sqrt{2(1 + \delta_{B_1 B_2})}} \{ [B_1 B_2]_{II_i} + \mathcal{P}(-1)^{I_1+I_2-I} [B_2 B_1]_{II_i} \} \\ &= \sqrt{\frac{2}{1 + \delta_{B_1 B_2}}} \sum_{(\lambda\mu)\rho \in \mathcal{P}} \langle (11)a_1(11)a_2 \parallel (\lambda\mu)a \rangle_{\rho} [B_{(11)}B_{(11)}]_{(\lambda\mu)\alpha;\rho}, \quad (2.5) \end{aligned}$$

where the sum is over  $(\lambda\mu)\rho$  compatible with Eq. (2.3). As is apparent from the construction, the basis in Eq. (2.5) is naturally an eigen-state of the flavor exchange operator  $P_{12}^F$  with the eigen-value  $\mathcal{P}$ .

It is now straightforward to incorporate the spin degree of freedom in the above formulation and extend the whole arithmetics to the spin-flavor  $SU_6$  wave functions of the  $(3q)$ - $(3q)$  system. In the quark model, the isospin basis of the spin-flavor functions is given by

$$\xi_{\alpha}^{SF} = \frac{1}{\sqrt{2(1 + \delta_{a_1 a_2})}} \left\{ \left[ W_{\frac{1}{2}(11)a_1}^{[3]}(123) W_{\frac{1}{2}(11)a_2}^{[3]}(456) \right]_{SS,II_z} \right. \\ \left. + \mathcal{P}(-1)^{I_1 + I_2 - I} \left[ W_{\frac{1}{2}(11)a_2}^{[3]}(123) W_{\frac{1}{2}(11)a_1}^{[3]}(456) \right]_{SS,II_z} \right\}, \quad (2.6)$$

where the totally symmetric  $SU_6$  wave function  $W_{S(\lambda\mu)a}^{[3]}(123)$  for the  $(3q)$  system<sup>18)</sup> is

$$W_{\frac{1}{2}(11)a}^{[3]}(123) = \sum_{S(\lambda\mu)=0(01), 1(20)} \frac{1}{\sqrt{2}} [ [ w_{\frac{1}{2}}(1) w_{\frac{1}{2}}(2) ]_S w_{\frac{1}{2}}(3) ]_{\frac{1}{2}} \\ \times [ [ F_{(10)}(1) F_{(10)}(2) ]_{(\lambda\mu)} F_{(10)}(3) ]_{(11)a} \quad (2.7)$$

with  $w_{\frac{1}{2}}$  being the spin wave function and  $F_{(10)}$  the flavor wave function. The subscript  $\alpha$  in Eq. (2.6) specifies a set of quantum numbers of the channel wave functions;

$$\alpha \equiv \left[ \frac{1}{2}(11)a_1, \frac{1}{2}(11)a_2 \right]_{SS_z Y I I_z; \mathcal{P}}. \quad (2.8)$$

The basis of Eq. (2.6) is the eigen-state of the core-exchange operator  $P_0^{SF} = P_{14}^{SF} P_{25}^{SF} P_{36}^{SF}$  with the eigen-value  $(-1)^{1-S}\mathcal{P}$ , where  $P_{ij}^{SF} = P_{ij}^g P_{ij}^f$  is the quark exchange operator in the spin-flavor space.

Table I shows the relationship between the isospin basis and the flavor- $SU_3$  basis given through Eq. (2.5) with respect to the  $NN$  and  $YN$  systems. In the following we always assume that the second particle is the nucleon, since we only discuss in this paper  $Y = Y_1 + Y_2 = 2$  and 1 cases. From this table we can obtain some interesting findings with respect to the characters of the  $YN$  interaction. For the flavor symmetric configuration with the singlet-even ( ${}^1E$ ) or the triplet-odd ( ${}^3O$ ) spin-space structure, the  $I = 1$  state of  $NN$  and the  $I = 3/2$  state of  $\Sigma N$  have the same  $SU_3$  content (22). Therefore, if the

Hamiltonian for the  $B_8$ - $B_8$  system is flavor singlet, both configurations yield exactly the same potential. Similarly,  $\Lambda N$  and  $\Sigma N(I = 1/2)$  interactions should be equal in the flavor antisymmetric configurations involving the triplet-even ( ${}^3E$ ) or the singlet-odd ( ${}^1O$ ) state, because the cross term contribution between  $(11)_a$  and  $(03)$   $SU_3$  states vanishes for the  $SU_3$ -scalar Hamiltonian. These features are, in fact, approximately observed in the phase-shift behavior of the OBEP's for the  $NN$  and  $YN$  interactions. Figure 1 shows the phase-shift behavior calculated with the central potentials of the Nijmegen model-F which fits well the  $NN$  phase shifts and the low-energy  $YN$  scattering data. As is expected, the  ${}^1S$  phase shifts of the  $NN$  and  $\Sigma N(I = 3/2)$  channels are both attractive and rather similar except for the low energy region. The difference of the  ${}^3S$  phase shifts of the  $\Lambda N$  and  $\Sigma N(I = 1/2)$  systems is within several degrees in the whole energy range. As is discussed in the introduction, the meson-baryon coupling constants in the Nijmegen potentials are constrained by the  $SU_3$  relations and the flavor symmetry is explicitly broken only through the hadron masses and possibly through hard-core radii. This means that even in the OBEP description the Hamiltonian is approximately  $SU_3$  scalar. In the quark model the FSB is naturally introduced through the fact that the strange quark mass  $m_s$  is heavier than the up-down quark mass  $m_{ud}$ . There is no other origin of the FSB, since gluons have no flavor degree of freedom. Thus, if we set the mass ratio  $\lambda = m_s/m_{ud}$  equal to unity and reduce the mass difference of octet baryons to zero, the above relations should be strictly satisfied in the present  $SU_6$  quark model.

The nice feature in the  $SU_3$  limit discussed above is not restricted to the central force. In the  $YN$  interaction, the spin value is not a conserved quantity unlike the  $NN$  system. The parity conservation in Eq. (2.4) shows that the transition from the spin  $S = 0$  to 1 or 1 to 0 is possible at the cost of the flavor-symmetry change, which leads to the well-known antisymmetric  $LS$  ( $LS^{(-)}$ ) force discussed in Ref. 13). However, the  $LS^{(-)}$  force for  $\Sigma N(I = 3/2)$  system connecting  ${}^3O$  and  ${}^1O$  states is very weak, since these states belong to the different  $SU_3$  symmetry (22) and (30), respectively. On the other hand, this is not the case for  $\Lambda N$  and  $\Sigma N(I = 1/2)$  systems, where very prominent contribution comes from the

cross term of  $(11)_s$  and  $(11)_a$  components with the same  $SU_3$  label  $(11)$ .

The  $SU_3$  contents of the  $YN$  systems are in fact widely employed in the literature for the discussion at the baryon level. For example, in the Nijmegen model-F the hard core radii are determined by assuming that they are the same within the same  $SU_3$  representations.<sup>3)</sup> This is rather plausible assumption to make, since the quark-model Hamiltonian are approximately flavor singlet. As a natural consequence, we can easily expect that the quark model potentials are more favorably compared with the model-F than with the model-D which does not have this constraint. This is indeed found to be the case in Ref. 13) for the  $LS$  and  $LS^{(-)}$  forces. The agreement between the quark-model potentials and the Nijmegen models is generally very reasonable. However, when the model-D and model-F give different predictions for the characteristic behavior, our quark model apparently supports the model-F. We will show in the following sections that the same situation is true for the central force of the  $YN$  interaction.

The  $SU_3$  symmetry is a natural symmetry in the quark-model description of the  $YN$  interaction, and it can be best studied if one starts from the symmetric quark Hamiltonian and introduces the FSB step by step. As the first step of such an approach, we discuss here an interesting correlation between the behavior of the central phase shifts in Fig. 1 and the spin-flavor-color factors of the exchange normalization kernel defined by

$$X_N = (-9)\frac{1}{3} \langle \xi_{\alpha}^{SF} | P_{36}^{SF} | \xi_{\alpha'}^{SF} \rangle . \quad (2.9)$$

As is well-known in the nuclear cluster study of light nuclei, the eigen-values of the normalization kernel is conveniently classified by the  $SU_3$  irreducible representations, which is nothing but the consequence of the  $SU_3$  scalar property of the antisymmetrization operator.<sup>19)</sup> If we neglect the small off-diagonal components with different cluster configurations  $\alpha \neq \alpha'$ , we can use  $X_N$  as a measure of attraction needed in each of the 16 phase shifts shown in Fig. 1. This idea is further prompted by observing the explicit expressions of the  $\mathbf{p} = 0$  Wigner transform for quark-exchange kernels given in Eq. (21) of Ref. 15) (See also Ref. 17).). If the FSB is neglected, all the spin-flavor factors of the quark central kernels are proportional to

$X_N$  except for the spin-dependent color-magnetic term. Therefore, it is indeed instructive to examine  $X_N$  in order to understand the gross features of the 16 spin-flavor states of the  $NN$  and  $YN$  systems. The behavior of central phase shifts shown in Fig. 1 is summarized in Table II together with the values of  $X_N$ . We find that, in each group of the even- and odd-state phase shifts, the larger value of  $X_N$  corresponds to the stronger attraction. In the even-parity states there are three cases with  $X_N = 1/9$  that correspond to the attractive phase shifts with the maximum values  $60^\circ$ ,  $36^\circ$  and  $19^\circ$  in  $NN \ ^1S$ ,  $\Sigma N(I = 3/2) \ ^1S$  and  $NN \ ^3S$  channels, respectively. In three  $X_N = 0$  cases, the maximum values are given by  $23^\circ$  for  $\Lambda N \ ^1S$ ,  $6^\circ$  for  $\Lambda N \ ^3S$  and  $4^\circ$  for  $\Sigma N(I = 1/2) \ ^3S$ . On the other hand, the strong repulsive phase shifts in  $\Sigma N(I = 1/2) \ ^1S$  and  $\Sigma N(I = 3/2) \ ^3S$  states have both large negative values  $-8/9$  and  $-7/9$ , respectively. In the odd parity states the effect of  $X_N$  is somewhat weakened due to the existence of the centrifugal barriers. Nevertheless, the same trend is almost apparent; i.e., the attractive phase shift up to  $70^\circ$  in  $\Sigma N(I = 3/2) \ ^1P$  and that up to  $9^\circ$  in  $\Sigma N(I = 1/2) \ ^3P$  have  $X_N = 1/3$  and  $5/27$ , respectively. The three states with  $X_N = -1$  correspond to the weak repulsion observed in  $\Lambda N \ ^3P$ ,  $\Lambda N \ ^1P$  and  $\Sigma N(I = 1/2) \ ^1P$ . These are almost degenerate with another group of  $NN \ ^3P$  and  $\Sigma N(I = 3/2) \ ^3P$  states, both of which have  $X_N = -31/27$ . Finally, the  $^1P$  state of the  $NN$  system gives particularly large negative value  $X_N = -7/3$  and the strong repulsion. Since the eigen-values of the normalization kernel in the single-channel systems with  $(0s)^6$  or  $(0s)^5(0p)$  configurations are given by  $\mu = 1 + X_N$  (for even-parity states) or  $\mu = 1 + (1/3) X_N$  (for odd-parity states), these features are nothing but the effect of the Pauli principle already discussed in Refs. 9) and 20) for the  $S$ -wave states.

The above analysis strongly indicates that, as long as the FSB is neglected, our quark-model description in terms of the Pauli principle and the short-range color-magnetic repulsion is on the right track for reproducing the gross features of the rich flavor dependence of the  $YN$  interaction. In order to succeed in complete reproduction of the central phase-shift behavior predicted by the Nijmegen potential, it might seem that one simply needs to supplement the present quark model with almost state-independent medium-range attraction.

We will see in the following sections that this is not entirely the case.

### III. FORMULATION OF THE MODEL

Since the RGM formalism for the  $(3q)$ - $(3q)$  system with simple harmonic-oscillator wave functions is rather standard, we will mainly discuss in this section a couple of new features that we need for an appropriate treatment of the c.m. motion in the Galilean non-invariant interaction and of the reduced mass.

The RGM wave function for the  $(3q)$ - $(3q)$  system can be written as

$$\Psi = \sum_{\alpha} \mathcal{A}' \{ \phi_{\alpha} \chi_{\alpha}(\mathbf{r}) \} \quad , \quad (3.1)$$

where the channel wave function  $\phi_{\alpha} = \phi^{(orb)} \xi_{\alpha}^{SF} \xi^C$  with  $\alpha$  being specified by Eq. (2.8) is composed of the spatial part of the internal wave function  $\phi^{(orb)} = \phi^{(orb)}(123)\phi^{(orb)}(456)$ , the color-singlet wave function  $\xi^C = C(123)C(456)$  and the isospin basis  $\xi_{\alpha}^{SF}$  of the spin-flavor  $SU_6$  wave functions defined by Eq. (2.6). The summation over  $\alpha$  in Eq. (3.1) is needed for the channel-coupling problem of  $\Lambda N$  and  $\Sigma N(I = 1/2)$  systems, which is not actually discussed in this paper. For  $\phi^{(orb)}(123)$  we adopt a simple  $(0s)^3$  configuration with a common harmonic-oscillator constant  $b$  and the c.m. motion is eliminated with the use of the usual definition of the c.m. coordinate  $\mathbf{X}_G = (\mathbf{x}_1 + \mathbf{x}_2 + \mathbf{x}_3)/3$ . Namely, the orbital function for the  $(3q)$  clusters is assumed to be flavor-independent and taken to be the same for all the octet baryons. The relative coordinate between the two clusters is denoted by  $\mathbf{r}$ . The antisymmetrization operator  $\mathcal{A}'$  in Eq. (3.1) makes  $\Psi$  totally antisymmetric under the exchange of quarks between the two  $(3q)$  systems and can be reduced to the simple form

$$\mathcal{A}' \longrightarrow \frac{1}{2}(1 - 9P_{36})(1 - P_0) \quad , \quad (3.2)$$

in practical calculations. It is normalized such that the normalization kernel approaches the unit operator in the limit of infinite cluster separation. The operator  $P_{36} = P_{36}^{(orb)} P_{36}^{SF} P_{36}^C$  exchanges the quarks 3 and 6, and  $P_0 = P_{14} P_{25} P_{36}$  is the core-exchange operator which

interchanges the two clusters as a whole. The relative-motion function  $\chi_{\alpha}(\mathbf{r})$  is assumed to be parity-projected in such a way that the parity is compatible with the spin value  $S$  and the flavor-symmetry phase  $\mathcal{P}$  through the generalized Pauli principle of Eq. (2.4);  $\chi_{\alpha}(-\mathbf{r}) = (-1)^S \mathcal{P} \chi_{\alpha}(\mathbf{r})$ .

Our quark interaction consists of a phenomenological quark confinement potential of the quadratic type and a one-gluon exchange potential of the Fermi-Breit interaction. For the kinetic-energy part we employ a simple non-relativistic expression,  $T_i = m_i + \mathbf{p}_i^2/2m_i$ , since the higher-order terms are absorbed to the redefinition of the reduced mass in the framework discussed in the next section. Thus the quark-model Hamiltonian we use for the  $(3q)$ - $(3q)$  system is expressed as

$$H = \sum_{i=1}^6 T_i + \sum_{i<j=1}^6 H_{qq}(i, j) \quad , \quad (3.3)$$

where the  $qq$  interaction  $H_{qq}$  is in general composed of the following pieces:<sup>15)</sup>

$$H_{qq} = U^{Cf} + U^{CC} + U^{MC} + U^{GC} + U^{sLS} + U^{aLS} + U^T \quad . \quad (3.4)$$

In Eq. (3.4), the superscript  $Cf$  stands for the confinement potential or the  $-(\lambda_1 \cdot \lambda_2) a_c r^2$  piece,  $CC$  for the color-coulombic or  $(\lambda_1 \cdot \lambda_2)/r$  piece,  $MC$  for the momentum-dependent retardation term or  $(\lambda_1 \cdot \lambda_2) \{ (\mathbf{p}_1 \cdot \mathbf{p}_2) + \mathbf{r}(\mathbf{r} \cdot \mathbf{p}_1) \cdot \mathbf{p}_2 / r^2 \} / (2m_1 m_2 r)$  piece,  $GC$  for the combined color-delta and color-magnetic or  $(\lambda_1 \cdot \lambda_2) \{ 1/(2m_1^2) + 1/(2m_2^2) + 2/(3m_1 m_2) (\boldsymbol{\sigma}_1 \cdot \boldsymbol{\sigma}_2) \} \delta(\mathbf{r})$  piece,  $sLS$  for the symmetric  $LS$ ,  $aLS$  for the antisymmetric  $LS$  and  $T$  for the tensor terms. Here  $\mathbf{r}$  is the relative coordinate between two quarks.

In Eq. (3.3) we note that the total kinetic-energy operator is not subtracted from the full Hamiltonian. In fact, this is purposely done, since the Galilean invariance is not respected in our formulation. As is discussed in the introduction, the appearance of the Galilean non-invariant terms is a direct consequence of the more strict Lorentz invariance at the relativistic level. We will also deal with these terms by calculating all the physical quantities at the total c.m. system. In the RGM formalism this can be done as follows. Let  $\mathcal{O}$  be any kind of many-body operators of the  $(3q)$ - $(3q)$  system, usually involving the derivative operators and permutations of quarks. The RGM kernel for  $\mathcal{O}$  at the c.m. system is calculated through

$$\begin{aligned}
& \langle \phi_\alpha \delta(\mathbf{r} - \mathbf{R}) | \mathcal{O} | \phi_{\alpha'} \delta(\mathbf{r} - \mathbf{R}') \rangle \equiv \langle \delta(\mathbf{X}_G) \phi_\alpha \delta(\mathbf{r} - \mathbf{R}) | \mathcal{O} | 1 \cdot \phi_{\alpha'} \delta(\mathbf{r} - \mathbf{R}') \rangle \\
& = \left( \frac{6\nu}{2\pi} \right)^{\frac{3}{2}} \int d\mathbf{a} \langle \Gamma_{6\nu}(\mathbf{X}_G, 0) \phi_\alpha \delta(\mathbf{r} - \mathbf{R}) | \mathcal{O} | \Gamma_{6\nu}(\mathbf{X}_G, \mathbf{a}) \phi_{\alpha'} \delta(\mathbf{r} - \mathbf{R}') \rangle , \quad (3.5)
\end{aligned}$$

where  $\Gamma_\gamma(\mathbf{X}, \mathbf{a}) = (2\gamma/\pi)^{3/4} \exp\{-\gamma(\mathbf{X} - \mathbf{a})^2\}$  and  $\mathbf{X}_G$  is the c.m. coordinate of the  $6q$  system.

As an example of the above prescription, we calculate the direct term of the kinetic-energy kernel in the momentum representation for the relative motion. For the mass dependence in  $T_i = m_i + \mathbf{p}_i^2/2m_i$ , we can use the relationship like

$$\frac{1}{m_i} = \frac{1}{m_{ud}} \left\{ \frac{1}{3} \left( 2 + \frac{1}{\lambda} \right) + \left( 1 - \frac{1}{\lambda} \right) Y_i \right\} , \quad (3.6)$$

in order to take into account the FSB explicitly. Here,  $\lambda = m_s/m_{ud}$  and  $Y_i$  is the hypercharge operator for the quark  $i$ . A straightforward calculation through Eq. (3.5) yields

$$\begin{aligned}
I_{\alpha\alpha'}^{(K)D}(\mathbf{k}, \mathbf{k}') & = \langle \delta(\mathbf{X}_G) \phi_\alpha e^{i\mathbf{k}\mathbf{r}} | \sum_{i=1}^6 T_i | 1 \cdot \phi_{\alpha'} e^{i\mathbf{k}'\mathbf{r}} \rangle \\
& = \delta_{\alpha\alpha'} (2\pi)^3 \delta(\mathbf{k} - \mathbf{k}') \left( E_{\alpha_1 \mathbf{k}}^{(K)} + E_{\alpha_2, -\mathbf{k}}^{(K)} \right) , \quad (3.7)
\end{aligned}$$

where  $E_{\mathbf{a}\mathbf{k}}^{(K)}$  is the energy of the  $3q$  system moving with the momentum  $\mathbf{k}$  and is given by

$$E_{\mathbf{a}\mathbf{k}}^{(K)} = E_a^{(K)} + \frac{\hbar^2}{2M_a^{(K)}} \mathbf{k}^2 \quad (3.8)$$

with

$$\begin{aligned}
E_a^{(K)} & = m_{ud} \left\{ [2 + \lambda + (1 - \lambda)Y] + \frac{x^2}{2} \left[ 2 + \frac{1}{\lambda} + \left( 1 - \frac{1}{\lambda} \right) Y \right] \right\} , \\
\frac{1}{M_a^{(K)}} & = \frac{1}{m_{ud}} \frac{1}{9} \left[ 2 + \frac{1}{\lambda} + \left( 1 - \frac{1}{\lambda} \right) Y \right] . \quad (3.9)
\end{aligned}$$

Here  $a = YI$  and the non-dimensional parameter  $x = (1/m_{ud}b)$  (which is almost always around 1) is employed. The transformation to the RGM kernel is easily carried out, yielding

$$\begin{aligned}
\mathcal{M}_{\alpha\alpha'}^{(K)D}(\mathbf{R}, \mathbf{R}') & = \langle \delta(\mathbf{X}_G) \phi_\alpha \delta(\mathbf{r} - \mathbf{R}) | \sum_{i=1}^6 T_i | 1 \cdot \phi_{\alpha'} \delta(\mathbf{r} - \mathbf{R}') \rangle \\
& = \delta_{\alpha\alpha'} \left[ \left( E_{\alpha_1}^{(K)} + E_{\alpha_2}^{(K)} \right) - \frac{\hbar^2}{2\mu_\alpha^{(K)}} \left( \frac{\partial}{\partial \mathbf{R}} \right)^2 \right] \delta(\mathbf{R} - \mathbf{R}') , \quad (3.10)
\end{aligned}$$

where  $\mu_\alpha^{(K)}$  is the reduced mass defined through  $1/\mu_\alpha^{(K)} = 1/M_{\alpha_1}^{(K)} + 1/M_{\alpha_2}^{(K)}$ .

The momentum-dependent retardation term  $U^{MC}$  in Eq. (3.4) can be similarly treated, since this term has the structure of the two-body kinetic-energy term. The energy of the  $3q$  system moving with the momentum  $\mathbf{k}$  is now given by

$$E_{\mathbf{a}\mathbf{k}}^{(MC)} = -\sqrt{\frac{2}{\pi}} \alpha_S x^3 m_{ud} \frac{2}{3} f_a^{MC} \left[ 1 - \frac{2}{9} (b\mathbf{k})^2 \right] , \quad (3.11)$$

where  $\alpha_S$  is the quark-gluon coupling constant and the spin-flavor factor  $f_a^{MC}$  normalized to unity for the nucleon is given by

$$f_a^{MC} = \frac{1}{3} \lambda^Y \left[ \left( 1 + \frac{2}{\lambda} \right) - \left( 1 - \frac{1}{\lambda} \right) Y \right] . \quad (3.12)$$

The direct term of the RGM kernel for  $\sum_{i < j=1}^6 U^{MC}(i, j)$  is given by

$$\mathcal{M}_{\alpha\alpha'}^{(MC)D}(\mathbf{R}, \mathbf{R}') = \delta_{\alpha\alpha'} \left( E_{\alpha_1}^{(MC)} + E_{\alpha_2}^{(MC)} \right) \left[ 1 + \frac{2}{9} b^2 \left( \frac{\partial}{\partial \mathbf{R}} \right)^2 \right] \delta(\mathbf{R} - \mathbf{R}') . \quad (3.13)$$

where  $E_a^{(MC)} = E_{\mathbf{a}, \mathbf{k}=0}^{(MC)}$  in Eq. (3.11). Thus the internal-energy contribution from the  $U^{MC}$  term is naturally defined through the expectation value at the rest frame. It is instructive to compare the result of Eq. (3.13) with the direct RGM kernels for the other pieces of the Fermi-Breit interaction;  $\Omega = Cf, CC$  and  $GC$ . These are given by

$$\mathcal{M}_{\alpha\alpha'}^{(\Omega)D}(\mathbf{R}, \mathbf{R}') = \delta_{\alpha\alpha'} \delta(\mathbf{R} - \mathbf{R}') \left( E_{\alpha_1}^{(\Omega)} + E_{\alpha_2}^{(\Omega)} \right) \quad \text{for } \Omega = Cf, CC \text{ and } GC . \quad (3.14)$$

By combining the results in Eqs. (3.10), (3.13) and (3.14), the direct part of the RGM kernel is given by

$$\mathcal{M}_{\alpha\alpha'}^D(\mathbf{R}, \mathbf{R}') = \delta_{\alpha\alpha'} \left[ \left( E_{\alpha_1}^{int} + E_{\alpha_2}^{int} \right) - \frac{\hbar^2}{2\mu_\alpha} \left( \frac{\partial}{\partial \mathbf{R}} \right)^2 \right] \delta(\mathbf{R} - \mathbf{R}') , \quad (3.15)$$

where the internal-energy contribution  $E_a^{int}$  and the reduced mass  $\mu_\alpha$  are given by

$$\begin{aligned}
E_a^{int} & = \sum_{\Omega=K, Cf, CC, MC, GC} E_a^{(\Omega)} , \\
\mu_\alpha & = \frac{3}{2} m_{ud} \left[ \frac{1}{3} \left( 2 + \frac{1}{\lambda} \right) + \frac{1}{6} \left( 1 - \frac{1}{\lambda} \right) Y + \sqrt{\frac{2}{\pi}} \alpha_S x \frac{4}{9} \left( f_{\alpha_1}^{MC} + f_{\alpha_2}^{MC} \right) \right]^{-1} . \quad (3.16)
\end{aligned}$$



If we set  $\lambda = 1$  and neglect the  $MC$  contribution in Eq. (3.16), we recover a simple result  $\mu_\alpha = (3/2)m_{ud}$ . The  $MC$  term has a role to reduce the value of  $\mu_\alpha$ .

We can now write down the RGM equation for the relative-motion function  $\chi_\alpha(\mathbf{r})$  as

$$\left[ \varepsilon_\alpha + \frac{\hbar^2}{2\mu_\alpha} \left( \frac{\partial}{\partial \mathbf{R}} \right)^2 \right] \chi_\alpha(\mathbf{R}) = \sum_{\alpha'} \int d\mathbf{R}' G_{\alpha\alpha'}(\mathbf{R}, \mathbf{R}') \chi_{\alpha'}(\mathbf{R}') . \quad (3.17)$$

where the relative energy  $\varepsilon_\alpha$  in the channel  $\alpha$  is related to the total energy  $E$  of the system through  $\varepsilon_\alpha = E - E_{a_1}^{int} - E_{a_2}^{int}$ , and the exchange kernel  $G_{\alpha\alpha'}(\mathbf{R}, \mathbf{R}')$  is given by

$$G_{\alpha\alpha'}(\mathbf{R}, \mathbf{R}') = \sum_{\Omega} \mathcal{M}_{\alpha\alpha'}^{(\Omega)}(\mathbf{R}, \mathbf{R}') - \varepsilon_\alpha \mathcal{M}_{\alpha\alpha'}^N(\mathbf{R}, \mathbf{R}') . \quad (3.18)$$

The summation in Eq. (3.18) is over  $\Omega = K, CC, MC, GC, sLS, aLS$  and  $T$  of Eq. (3.4), among which the central components  $\Omega = K, CC, MC$  and  $GC$  need subtraction of the internal-energy contributions through

$$\mathcal{M}_{\alpha\alpha'}^{(\Omega)}(\mathbf{R}, \mathbf{R}') = \mathcal{M}_{\alpha\alpha'}^{(\Omega)exch}(\mathbf{R}, \mathbf{R}') - (E_{a_1}^{(\Omega)} + E_{a_2}^{(\Omega)}) \mathcal{M}_{\alpha\alpha'}^N(\mathbf{R}, \mathbf{R}') . \quad (3.19)$$

In Eqs. (3.18) and (3.19)  $\mathcal{M}_{\alpha\alpha'}^N(\mathbf{R}, \mathbf{R}')$  and  $\mathcal{M}_{\alpha\alpha'}^{(\Omega)exch}(\mathbf{R}, \mathbf{R}')$  are the exchange normalization and interaction (of the type  $\Omega$ ) kernels, respectively, and the internal energies are subtracted in the prior form. The exchange kernel in Eq. (3.19), which is derived analytically for each piece of the interaction, has the advantage that it is free from the internal-energy contribution. In particular, the mass term of the kinetic-energy operator  $T_i$  and the confinement potential with  $\Omega = Cf$  exactly cancel out between the exchange part and the internal-energy contribution in Eq. (3.19). We consider the latter feature one of the advantages of the present RGM formalism, in which the baryon-baryon interaction is independent of the strength of the confinement potential and is insensitive to the details of the confinement phenomenology.

In order to apply the WKB-approximation<sup>16)</sup> to the RGM equation in Eq. (3.17), we need to simplify the present coupled-channel formulation by neglecting the  $\Delta N$ - $\Sigma N$  ( $I = 1/2$ ) channel-coupling effect and the noncentral forces. The single-channel exchange kernel  $G_{\alpha\alpha}(\mathbf{R}, \mathbf{R}')$  for the  $(3q)$ - $(3q)$  system is converted to the corresponding Wigner transform through

$$G_{\alpha\alpha}^W(\mathbf{R}, \mathbf{P}) = \int d\mathbf{s} e^{i\mathbf{s}\cdot\mathbf{P}} G_{\alpha\alpha} \left( \mathbf{R} - \frac{\mathbf{s}}{2}, \mathbf{R} + \frac{\mathbf{s}}{2} \right) . \quad (3.20)$$

The effective local potential,  $U_\alpha^{eff}(R)$ , follows from  $G_{\alpha\alpha}^W(\mathbf{R}, \mathbf{P}) \equiv G_{\alpha\alpha}^W(R^2; \mathbf{P}^2; (\mathbf{R}\cdot\mathbf{P})^2)$  via the transcendental equation

$$U_\alpha^{eff}(R) = G_{\alpha\alpha}^W \left( R^2 ; 2\mu_\alpha [\varepsilon_\alpha - U_\alpha^{eff}(R)] ; 2\mu_\alpha R^2 [\varepsilon_\alpha - U_\alpha^{eff}(R)] - \hbar^2 \left( L + \frac{1}{2} \right)^2 \right) , \quad (3.21)$$

where  $L=0$  or  $1$  for  $S$ - or  $P$ -wave.

#### IV. A SIMPLE ANALYSIS BY SAITO MODEL

The effect of the Pauli principle on the interaction between composite particles was first studied by Saito in the case of the interaction between two  $\alpha$ -particles.<sup>21)</sup> What he found is that, the most important role of the Pauli principle is taken into account as the orthogonality condition on the relative motion with respect to the Pauli-forbidden states. This leads to the almost energy-independent nodal behavior of the relative-motion function in the overlapping region, which is interpreted as the origin of the phenomenological repulsive core. To demonstrate the essence of this Pauli effect, Saito calculated the  $S$ -wave phase shift in the RGM framework by retaining only the exchange kinetic-energy kernel. The resulting phase shift at the low incident energies has shown such a behavior as is expected from the hard-sphere scattering.

In this section we apply the Saito model to the  $(3q)$ - $(3q)$  system, and try to see if the qualitative analysis in Section 2 can be extended to more realistic situation in which some of the quark exchange kernels with the FSB is explicitly incorporated. We solve the RGM equation with all the  $qq$  interactions turned off, except for the  $U^{MC}$  term which gives the large contribution to the reduced-mass term. Since the inertia mass is not correctly reproduced in the usual non-relativistic quark model, it is essential to introduce a nice prescription to reproduce the correct kinematics for the baryon-baryon scattering in such a way that the reduced mass becomes exactly the empirical value, the Pauli principle is strictly respected

and the flavor-symmetry content of each system is well reserved even in the realistic case with the FSB. For the single-channel systems the above requirement is satisfied by multiplying the Saito equation by the factor  $\mu_\alpha/\mu_\alpha^{exp}$  with  $\mu_\alpha^{exp}$  being the empirical reduced mass, and by redefining  $\varepsilon_\alpha\mu_\alpha/\mu_\alpha^{exp}$  as the physical relative energy  $\tilde{\varepsilon}_\alpha$  corresponding to the wave number  $k_\alpha$  through  $\tilde{\varepsilon}_\alpha = (\hbar^2 k_\alpha^2/2\mu_\alpha^{exp})$ . The Saito equation we solve is given by

$$\left[ \tilde{\varepsilon}_\alpha + \frac{\hbar^2}{2\mu_\alpha^{exp}} \left( \frac{\partial}{\partial \mathbf{R}} \right)^2 \right] \chi_\alpha(\mathbf{R}) = \int d\mathbf{R}' \left\{ \frac{\mu_\alpha}{\mu_\alpha^{exp}} \left[ \mathcal{M}_{\alpha\alpha}^{(K)}(\mathbf{R}, \mathbf{R}') + \mathcal{M}_{\alpha\alpha}^{(MC)}(\mathbf{R}, \mathbf{R}') \right] - \tilde{\varepsilon}_\alpha \mathcal{M}_{\alpha\alpha}^N(\mathbf{R}, \mathbf{R}') \right\} \chi_\alpha(\mathbf{R}') . \quad (4.1)$$

In other words, what we need is to replace the exchange kernel  $\mathcal{M}_{\alpha\alpha}^{(K)}(\mathbf{R}, \mathbf{R}')$  and  $\mathcal{M}_{\alpha\alpha}^{(MC)}(\mathbf{R}, \mathbf{R}')$  in Eqs. (3.17) and (3.18) by

$$\tilde{\mathcal{M}}_{\alpha\alpha}^{(\Omega)}(\mathbf{R}, \mathbf{R}') = \frac{\mu_\alpha}{\mu_\alpha^{exp}} \mathcal{M}_{\alpha\alpha}^{(\Omega)}(\mathbf{R}, \mathbf{R}') \quad \text{for } \Omega = K \text{ and } MC . \quad (4.2)$$

and at the same time to use the empirical reduced mass for  $\mu_\alpha$  and the physical relative energy for  $\varepsilon_\alpha$  in Eq. (3.17).

Before solving Eq. (4.1), we give the input parameters used in our model. The input parameters of our model consist of the harmonic-oscillator constant  $b$ , the up-down quark mass  $m_{ud}$ , the quark-gluon coupling constant  $\alpha_S$  and the ratio of the strange to up-down quark mass  $\lambda = m_s/m_{ud}$ . The quadratic-type confinement potential has a special feature that it does not contribute to the exchange kernel. We may take any arbitrary value for the strength of the confinement potential. The numerical values of the other parameters are

$$b = 0.6 \text{ fm}, \quad m_{ud} = 313 \text{ MeV}, \quad \alpha_S = 1.5187, \quad \lambda = 1.25 , \quad (4.3)$$

where the value of  $\alpha_S$  is determined so as to reproduce the  $N$ - $\Delta$  mass splitting correctly through the color-magnetic term : i.e.,  $\sqrt{2/\pi}\alpha_S x^3 m_{ud} = 440 \text{ MeV}$ .<sup>13)</sup> Since our purpose is not to find the best fit to the experiment but to understand the global structure of the phase-shift behavior in the  $NN$  and  $YN$  systems, the above standard values of  $b$ ,  $m_{ud}$ , and  $\alpha_S$  are fixed in the following discussion. The value of  $\lambda$  is tentatively chosen to be 1.25 unless otherwise specified. From the study of hadron spectroscopy assuming the pure (3q)

configuration, the strange quark mass is estimated to be about 150 MeV heavier than the up-down quark mass, which leads to the value around  $\lambda=1.6$ . The mesonic effect is expected to reduce the value of  $\lambda$  into around  $\lambda = 1.25$ .<sup>15)</sup> With the quark parameters in Eq. (4.3) the reduced mass  $\mu_\alpha$  of Eq. (3.16) for the  $\Sigma N$  system, for example, turns out to be 232 MeV, which is only half of the empirical reduced mass  $\mu_\alpha^{exp}=525 \text{ MeV}$ . If the  $U^{MC}$  term is turned off, the calculated value  $\mu_\alpha$  would be 485 MeV, which is still smaller than the empirical value by 40 MeV. As a general feature of the present quark model, both kinetic-energy and momentum-dependent terms have almost the same order of magnitude in the contribution to the reduced mass, resulting in a rather pathological situation where the calculated reduced mass  $\mu_\alpha$  is significantly smaller than the empirical mass. From the explicit expression in Eq. (3.16), one may think that this difficulty can be overcome by assuming almost twice of the present up-down quark mass. This spoils, however, the simple picture of interacting non-relativistic quarks nicely built so far in describing the hadron structure and various low-energy hadron phenomena.

Fortunately, the above prescription largely cures this situation. In order to demonstrate that this procedure indeed yields a very reasonable result, we compare in Table III the  $S$ -wave phase shifts calculated for three typical groups with different  $X_N$  values: namely, attractive ones with  $X_N = 1/9$ , almost zero with  $X_N = 0$  and repulsive ones with  $X_N = -8/9$ . In this table the columns denoted by  $\tilde{K} + \tilde{MC}$  indicate results including both exchange kinetic-energy and  $U^{MC}$  terms. To examine the  $\lambda$ -dependence of the phase shifts, we here purposely employ two extreme values,  $\lambda=1$  and  $\lambda=1.69$ . The latter value was chosen in our previous study of the  $YN$  spin-orbit forces.<sup>13)</sup> The columns denoted by  $\tilde{K}$  indicate that the  $U^{MC}$  interaction is also turned off. We find from Table III useful information concerning the roles of the  $U^{MC}$  term and the effect of the FSB in the exchange kinetic-energy and  $U^{MC}$  kernels. First of all it is remarkable that the effect of the  $U^{MC}$  term is rather moderate in spite of the large variety of the factor  $\zeta = \mu_\alpha/\mu_\alpha^{exp}$  from about 0.4 to 1. The value one in the  $NN$  case is simply because we have chosen the up-down quark mass as just one third of the nucleon mass. In the  $NN$  system with  $X_N = 1/9$  the effect of the  $U^{MC}$  interaction

is to reduce the attractive phase-shift values at most by  $2 \sim 3$  degrees. On the other hand, in the repulsive phase shift in the  $\Sigma N(I = 1/2) {}^1S$  state with  $X_N = -8/9$ , the  $U^{MC}$  term plays the role of reducing the repulsion a little bit; i.e., about 5 degrees in the phase shifts at  $p_{lab} = 600$  MeV/c, for instance. This feature of reducing the Pauli repulsion turns out to be favorable in the more complete calculation including the other quark-model kernels and the effective meson-exchange potentials, since the Pauli repulsion of the quark-model potentials is usually too strong. However, the most prominent feature of the present prescription is in fact its amazing stability with respect to the introduction of the momentum-dependent non-Galilean-invariant term  $U^{MC}$ . Quite clearly, this is because the contribution of the exchange kernel  $\mathcal{M}_{\alpha\alpha}^{(MC)}(\mathbf{R}, \mathbf{R}')$  in Eq. (4.1) is largely cancelled by the change of  $\mu_\alpha/\mu_\alpha^{exp}$  which results from the exact treatment of the direct contribution under the same approximation. Now it is almost apparent that, even if we introduce the higher-order terms of the relativistic corrections in the single-particle kinetic-energy operator, such a effect should be rather minor as long as we deal with the direct term and the exchange term consistently.

We also stress that the present prescription is suited to study the FSB since it is based on the strict RGM formulation where the reduced mass is calculated from the same Hamiltonian. This means that, if we set  $\lambda = 1$  and choose the same incident wave number  $k_\alpha$ , the degenerate  $SU_3$  state like (22) in  $NN {}^1S$  and  $\Sigma N(I = 3/2) {}^1S$  channels yields exactly the same values of the phase shift, in spite of the fact that we use the experimental reduced mass. The small discrepancy of the phase-shift values between  $NN {}^1S$  and  $\Sigma N(I = 3/2) {}^1S$  channels with  $\tilde{K} + \tilde{M}C$  and  $\lambda = 1$  in Table III merely implies small difference of the incident c.m. momentum  $\mathbf{k}_\alpha$  between these two channels. We can thus study the effect of the FSB by changing the value of  $\lambda$  from unity to a some appropriate value while fitting the calculated reduced mass to the correct empirical mass. In fact, the effect of the FSB in the exchange kinetic-energy and momentum-dependent kernels themselves is usually rather moderate as is seen from Table III, except for just one case. This exception includes  $\Lambda N {}^1S$  and  ${}^3S$  channels with  $X_N = 0$ , in which the null phase-shift value at  $\lambda = 1$  decreases to about  $-6$  degrees at  $p_{lab} = 400$  MeV/c. The other phase shifts in  $\Sigma N(I = 3/2) {}^1S$  and  $\Sigma N(I = 1/2)$

${}^3S$  states gain weak attraction of the order of a couple of degrees as  $\lambda$  increases. However, this does not mean that the effect of the FSB is weak in these channels when the other quark-model potentials and the effective meson-exchange potentials are incorporated. In this realistic situation, we will find in the next section that the effect of the large empirical reduced mass in the  $\Sigma N$  channel makes the phase shift of the  $\Sigma N(I = 3/2) {}^1S$  channel strongly attractive compared with that of the  $NN {}^1S$  channel, when a common effective meson-exchange potential is introduced.

We show in Fig. 2 the 16 phase-shift curves calculated in the Saito model with the value of  $\lambda$  set equal to unity and with the  $U^{MC}$  term turned off. In this particular case the model becomes entirely parameter-free except for just one parameter  $b$ . As is already discussed with Table III, characteristic behavior shown here is almost preserved even if we incorporate the  $U^{MC}$  term and use the more realistic value  $\lambda = 1.25$ . Since there is no need to repeat the characteristic features of the phase-shift behavior discussed in Section II, we give here only a couple of comments related to the nature of the FSB observed in each system.

First, in the even-parity states of the  $NN$  system it is interesting to note that the Pauli effect works attractively, since the eigen-value of the normalization kernel is  $10/9$  which exceeds unity. Thus the repulsion comes from the color-magnetic interaction for the even partial waves, while it comes from the Pauli principle for the odd partial waves. Furthermore the degeneracy of the  ${}^1S$  and  ${}^3S$  states in the Saito model is quite accidental, since they belong to the different  $SU_3$  representations (22) and (03), respectively. In fact the effect of the color-magnetic interaction splits this degeneracy, but in the opposite direction to the one expected in the empirical phase shifts in Fig. 1. This causes a serious problem that we cannot use a common attractive potential even for the  $NN$  system. We have to introduce stronger attraction for the  ${}^1S$  state than the  ${}^3S$  state.

The next difficulty shows up in the  $\Sigma N(I = 3/2) {}^1S$  channel. Since the  $SU_3$  content of this channel is (22) and is the same as that of the  $NN {}^1S$  channel, the spin-flavor-color factors of the color-magnetic interaction for these channels are the same as long as we assume  $\lambda = 1$ . This implies that a common central attractive potential for these channels with

different reduced masses inevitably leads to more attractive phase-shift behavior for the  $\Sigma N(I = 3/2)^1S$  channel than that for the  $NN^1S$  channel, which is again in the opposite direction to the behavior in Fig. 1.

A similar situation to the one discussed above is also observed in the  $\Lambda N^3S$  and  $\Sigma N(I = 1/2)^3S$  channels. As is seen in Table I, these are the combinations of  $(11)_a$  and  $(03) SU_3$  states with the equal weight but the opposite sign. Therefore, if we again assume the  $SU_3$  limit and a common attractive potential, the  $\Sigma N$  channel should give slightly larger attraction in the phase shift than the  $\Lambda N$  channel does, since the reduced mass in the  $\Sigma N$  channel is slightly larger than that of the  $\Lambda N$  channel. This direction is further amplified by the FSB already discussed in Table III and also by that contained in the exchange kernel of the color-magnetic term  $U^{GC}$  in Eq. (3.4). Apparently, this is the opposite direction to the phase-shift behavior seen in Fig. 1. There the  $\Lambda N^3S$  phase shift is slightly more attractive than that of the  $\Sigma N(I = 1/2)^3S$  system, although the difference is less than 5 degrees. We should not overtrust the predictions by the central potentials of the Nijmegen model-F, since these phase shifts should be modified by the noncentral (mainly tensor) forces and the  $\Lambda N$ - $\Sigma N(I = 1/2)$  transition potentials. In general, the model-F introduces stronger  $\Lambda N$ - $\Sigma N(I = 1/2)$  coupling than the model-D does, so that the central phase shifts of the present channels predicted by the model-D are about 11 ~ 12 degrees more attractive than the corresponding ones in Fig. 1. Nevertheless, they are very much degenerate. This implies that it is very dangerous to conclude that the FSB is negligible even if the two phase-shift curves with the same  $SU_3$  content are almost equal to each other. We need careful examinations of the FSB not only in the whole quark-model potentials, but also in the effective meson-exchange potentials introduced by hand in the next section.

Finally a short comment follows as to the  $P$ -wave phase shifts. Due to the centrifugal barrier effect, the role of the FSB in the odd partial waves is generally rather modest.<sup>13)</sup> We can therefore safely discuss the effect of each component of the exchange kernels in the  $SU_3$  limit of  $\lambda = 1$ . In Fig.2 the  $\Sigma N(I = 3/2)^1P$  phase shift is more attractive than that of the  $\Sigma N(I = 1/2)^3P$  state corresponding to  $X_N = 1/3$  and  $X_N = 5/27$ , respectively. However,

once the exchange kernel of the  $U^{GC}$  term is incorporated, it turns out that the latter one becomes more attractive than the former one.

In summary, the present prescription is the most favorable one to study the FSB in the RGM framework. We remark that the momentum-dependent retardation term  $U^{MC}$  is treated differently from the other pieces of the Fermi-Breit interaction. We believe that this is inevitable if we try to extend the non-relativistic RGM framework to the basically relativistic system by retaining many nice features of the RGM. The most important finding in this section is that the present quark model can explain the basic features of the  $NN$  and  $YN$  phase-shift behavior even in its simplest version of the Saito model. We stress that this clearly reveals the essential role of the Pauli principle and that the proper treatment of the reduced mass as is done here is of prime importance to extract reliable and useful information.

## V. A REALISTIC ANALYSIS WITH EFFECTIVE MESON-EXCHANGE POTENTIALS

Before proceeding to detailed discussions of the effective attractive potentials needed for the realistic description of the  $NN$  and  $YN$  interaction, we briefly summarize the characters of the quark-model potentials except for those discussed in the preceding section. As to the central potentials, these are the ones from the color-Coulombic term  $U^{CC}$  and the color-magnetic contact term  $U^{GC}$ . The color-Coulombic term does not play any important role in the baryon-baryon interaction, since this piece of interaction is just a small modification of the confinement potential with respect to the radial form. On the other hand, the spin-dependent color-magnetic term is the origin of the short-range repulsion of the  $NN$  interaction especially for the even-parity states. We therefore only need to discuss the spin-flavor dependence of this repulsion for various channels of the  $NN$  and  $YN$  systems. The values of the Wigner transform with  $\mathbf{P} = 0$  and  $\lambda = 1$  at the most important distance  $|\mathbf{R}| = 1$  fm are classified into three groups for each parity state, depending on the magni-

tudes of the repulsion. The  $NN^1S$ ,  $\Sigma N(I = 3/2)^{1,3}S$  and  $\Lambda N^1S$  channels have 60 ~ 70 MeV, the  $NN^3S$  has 38 MeV, and the  $\Sigma N(I = 1/2)^{1,3}S$  and  $\Lambda N^3S$  have about 20 MeV. The  $NN^{1,3}P$ ,  $\Sigma N(I = 3/2)^3P$  and  $\Lambda N^3P$  have 60 ~ 80 MeV, the  $^1P$  states of  $\Lambda N$  and  $\Sigma N(I=1/2$  and  $3/2)$  have 30 ~ 45 MeV, and the  $\Sigma N(I = 1/2)^3P$  has only 8 MeV. From this comparison we can confirm that the splitting of the  $NN^1S$ ,  $^3S$ , and  $\Sigma N(I = 3/2)^1S$  phase shifts shown in Fig. 1 is not possible if we dwell on a common attractive potential, the finding already discussed in the preceding section.

Next we discuss the effective attractive potentials adopted in this investigation. As is already discussed in the introduction, we generate the effective local potentials  $V^{eff}$  through the meson-exchange potentials between quarks without calling for their microscopic origin and foundations. The reason for doing this is of course to reduce the number of parameters introduced in these phenomenological ingredients, and to gain the insight into the minimum augmentation of the effective meson-exchange potentials. It has also an advantage that we can use the rich knowledge accumulated so far with respect to the roles of mesons with full of variety. For example, the OBEP's for the  $NN$  interaction are generally characterized by the scalar-mesons responsible for the medium-range attraction, the pseudo-scalar mesons for the tensor and spin-spin central forces, and the vector mesons for the short-range repulsion and the spin-orbit force. Among these the effect of vector mesons is particularly short-ranged and is expected to be accounted for by the quark-model potentials. We have examined the spin-spin central components predicted by the quark-model potentials in the present Wigner-transform RGM techniques, and found that they have very nice flavor dependence similar to that of the Nijmegen model-F potentials with respect to the  $NN$  and  $YN$  systems. We therefore omit vector mesons with the reservation that they may somehow modify the conclusion obtained by using only the scalar and pseudo-scalar mesons. Furthermore, the effect of spin-spin part of the pseudo-scalar mesons is rather weak compared with the very strong central force afforded by the scalar mesons. Although the spin-spin part of the long-range one-pion exchange potential is of course very important in the detailed description of the low-energy phase shifts in high partial waves, we consider that the incorporation of this

type of component is the next step to refine the present result. After all, we adopt only the spin-independent central force originating from the scalar mesons, in order to make a step toward the understanding of the basic features of the central attraction for the  $NN$  and  $YN$  systems.

The effective local meson-exchange potential is constructed by folding the OBEP with the density distribution of the  $(3q)$  clusters, which is equivalent to using the form factor  $\exp\{-(b\mathbf{q})^2/6\}$  in the momentum space. Then  $V_\beta^{eff}$  of the  $BN$  channel for a scalar meson  $\beta = \epsilon, S^*, \delta$  or  $\kappa$  with the mass  $m_\beta$  is given by

$$V_\beta^{eff}(\mathbf{R}) = - \left\{ \begin{array}{l} f_{BB\beta} f_{NN\beta} \\ f_{BN\beta} f_{BN\beta} \end{array} \right\} m_\beta Y_{\alpha_0}(x) \quad \text{for} \quad \left\{ \begin{array}{l} \beta = \epsilon, S^*, \delta \\ \beta = \kappa \end{array} \right. \quad (5.1)$$

where  $x = m_\beta |\mathbf{R}|$ ,  $\alpha_0 = (m_\beta b)^2/3$  and  $Y_\alpha(x)$  is the modified Yukawa function defined by

$$Y_\alpha(x) = \frac{e^\alpha}{2x} \left\{ e^{-x} \left[ 1 + \operatorname{erf} \left( \frac{x}{2\sqrt{\alpha}} - \sqrt{\alpha} \right) \right] - e^x \left[ 1 - \operatorname{erf} \left( \frac{x}{2\sqrt{\alpha}} + \sqrt{\alpha} \right) \right] \right\}. \quad (5.2)$$

As is seen from Eq. (5.2), the asymptotic behavior of  $Y_\alpha(x)$  for  $x \rightarrow \infty$  is not the simple Yukawa function  $Y(x) \equiv Y_0(x) = e^{-x}/x$  but  $e^\alpha Y(x)$ . The factor  $e^\alpha$  becomes fairly large for heavy mesons; for example, it increases from 1.06 for  $\pi$  to about 6 for  $\epsilon$  meson with the mass  $m_\epsilon \sim 760$  MeV. This factor is sometimes absorbed into the definition of the coupling constants, in order to ensure the correct asymptotic behavior of the one-pion exchange potential with the empirically determined value of the  $NN\pi$  coupling constant.<sup>7)</sup> We, however, keep this factor as it is, since in any case the overall strength of the effective meson-exchange potentials should be readjusted to reproduce the  $NN$  phase shifts.

In Eq. (5.1), the formulation is given for any kind of mesons of the scalar-meson nonet components, and  $f_{BB'\beta}$  are the baryon-meson coupling constants determined from the standard  $SU_3$  relations. The reason why we have to use the scalar-meson nonet as in the Nijmegen model-F is almost clear from the discussion given at the last part of the preceding section. The introduction of only the flavor-singlet  $\epsilon$  meson as in the Nijmegen model-D cannot reproduce the characteristic features of the  $NN$  and  $YN$  phase-shift behavior shown in Fig. 1. In fact, if we introduce the central attraction generated from the  $\epsilon$  meson of the

model-D and adjust the strength to fit the  $NN$   $^1S$  phase shift following the procedure described below, we find that the same attraction applied to the  $\Sigma N(I = 3/2)$   $^1S$  channel gives the phase-shift values of  $61.7^\circ$  for  $\lambda=1$  and  $70.4^\circ$  for  $\lambda=1.25$  at  $p_{lab} = 200$  MeV/c, which is too large as is seen from Fig. 1. The increase of the attraction from  $\lambda = 1$  to  $\lambda = 1.25$  is due to the weakening of the repulsion of the color-magnetic term. To seek a central attractive potential with suitable flavor dependence, we inevitably need to employ the OBEP with the scalar-meson nonet. We show in the following that the scalar-meson nonet of the Nijmegen model-F potential gives exactly the desired feature. To determine the coupling constants  $f_{BB'\beta}$  through the  $SU_3$  relations, we need four  $SU_3$  parameters,  $\alpha$  (the F/F+D ratio),  $\theta$  (the mixing angle between singlet and octet isoscalar mesons),  $f_1$  (the singlet coupling constant) and  $f_8$  (the octet coupling constant). These parameters and the meson masses  $m_\beta$  are taken from the Nijmegen model-F without any alteration.

We first determine the effective local potential by solving the transcendental equation given in Eq. (3.21) and then calculate the phase shifts with this potential. The Wigner transform of the exchange kernel of Eq. (3.20), for the single-channel RGM equation with the modification of the effective meson-exchange potentials is given by

$$G_{\alpha\alpha}^W(\mathbf{R}, \mathbf{P}) = \tilde{G}_{\alpha\alpha}^{(K)W}(\mathbf{R}, \mathbf{P}) + \tilde{G}_{\alpha\alpha}^{(MC)W}(\mathbf{R}, \mathbf{P}) + G_{\alpha\alpha}^{(CC)W}(\mathbf{R}, \mathbf{P}) + G_{\alpha\alpha}^{(GC)W}(\mathbf{R}, \mathbf{P}) - \varepsilon_\alpha G_{\alpha\alpha}^{(N)W}(\mathbf{R}, \mathbf{P}) + C_{\mathcal{P}} \left( \sum_{\beta} V_{\beta}^{eff}(\mathbf{R}) \right) \left( 1 + G_{\alpha\alpha}^{(N)W}(\mathbf{R}, \mathbf{P}) \right) . \quad (5.3)$$

where the summation of  $\beta$  is over  $\epsilon$ ,  $S^*$ ,  $\delta$  and  $\kappa$ . The multiplicative factor  $C_{\mathcal{P}}$  controls the balance of the interaction between the  $(3q)$ - $(3q)$  quark-model contribution and the effective meson-exchange contribution. It is chosen to be the same for all the nonet mesons but may depend on the flavor symmetry phase  $\mathcal{P}$ . This flavor-symmetry dependence turns out to be inevitable to simultaneously fit the central phase shifts of the  $^1S$  and  $^3S$  states of the  $NN$  system with the effective meson-exchange potentials generated only from the scalar mesons. Furthermore, a better fit of the phase shifts is obtained by allowing a slight energy-dependence in  $C_{\mathcal{P}}$ . In general, the effective meson-exchange potentials constructed by the folding procedure turns out to be fairly attractive at the short distances, and to

reduce the repulsion of the quark model significantly. The physical reason for weakening the contribution of the mesonic part by this energy-dependence is that the short-range part described by the quark model must be more important as the energy increases. The parameters of  $C_{\mathcal{P}}$  determined by fitting the  $S$ -wave phase shifts ( $^1S$  and  $^3S$ ) of the  $NN$  system are

$$C_1 = 0.56 e^{-\frac{1}{6}(b\mathbf{k})^2} , \quad C_{-1} = 0.33 e^{-\frac{1}{6}(b\mathbf{k})^2} , \quad (5.4)$$

where  $\mathbf{k}^2 = (2\mu_\alpha \varepsilon_\alpha / \hbar^2)$  with  $\mu_\alpha$  being the empirical reduced mass.

Since the nonlocal RGM kernel of the form  $\sqrt{N} V^{eff} \sqrt{N}$  is reduced to the algebraic multiplication in the WKB-approximation, we can dispense with the complexity arising from the square root of the normalization kernel. This WKB-RGM formalism further enable us to define the phase-shift equivalent local potentials, if the solution of the transcendental equation is obtained. It sometimes happens, however, that a real solution cannot be obtained because the local momentum turns into complex.<sup>17)</sup> This usually takes place when the repulsion due to the effect of the Pauli principle is too strong and the semi-classical approximation fails to simulate such purely quantum-mechanical phenomena. Due to this restriction, the numerical result will be shown below only for the following  $NN$  and  $YN$  channels; i.e.,  $NN$   $^1,3S$ ,  $\Lambda N$   $^1,3S$ ,  $\Sigma N(I = 3/2)$   $^1S$ ,  $\Sigma N(I = 3/2)$   $^1P$  and  $\Sigma N(I = 1/2)$   $^3P$  channels.

Figure 3 displays the  $S$ - and  $P$ -wave phase shifts calculated in the WKB-RGM formalism with respect to these solvable cases. The  $^1S$  phase shifts of the flavor-symmetric channels are generally in good agreement with the predictions by the Nijmegen model-F. Owing to the  $SU_3$  relations of the coupling constants and the singlet-octet meson mixing, the splitting of the  $NN$  and  $\Sigma N(I = 3/2)$  phase shifts is naturally explained. In addition to this, the  $\Lambda N$  phase shift has the right order of magnitude without any adjustment of the parameters. In the case of  $^3S$  states the phase-shift difference between the  $NN$  and  $\Lambda N$  systems agrees well with the prediction of the Nijmegen model, although the fall-off of the phase shifts at high energies is still a little too slow. Since these channels are subject to be improved by the tensor force, we postpone the detailed discussion of the energy dependence. The equivalent

local potential for the  $\Sigma N(I = 1/2) {}^3S$  channel cannot be obtained for  $\lambda = 1.25$ . However, if we choose a little smaller value  $\lambda = 1.1$ , we can obtain a solution of the transcendental equation. The resultant phase shifts calculated with this potential agree with those of the  $\Lambda N {}^3S$  channel within a few degrees and show slightly more repulsive behavior than the latter in accordance with the Nijmegen result.

In contrast to the  $S$ -wave cases, there arises a conspicuous difference in the behavior of the  $P$ -wave phase shifts between the present model and the Nijmegen model, especially in the  $\Sigma N(I = 3/2) {}^1P$  channel. The  $\Sigma N(I = 1/2) {}^3P$  phase shift indicates that the potential in this channel is more attractive than that in the  $\Sigma N(I = 3/2) {}^1P$  channel. This is opposite to the phase-shift behavior shown in Fig. 2, where only the effect of the Pauli principle is incorporated through the kinetic-energy type exchange kernels. This inversion took place from two reasons. The first one is that the repulsion from the color-magnetic term is stronger in the  $\Sigma N(I = 3/2) {}^1P$  channel than in the  $\Sigma N(I = 1/2) {}^3P$  channel, as is shown in the beginning of this section. The second reason is that the central attraction from the effective meson-exchange potentials is stronger in  $\Sigma N(I = 1/2) {}^3P$  channel than in  $\Sigma N(I = 3/2) {}^1P$  channel, since  $C_1$  is larger than  $C_{-1}$ . On the other hand, the Nijmegen model-F suggests that the potential in the  $\Sigma N(I = 3/2) {}^1P$  channel is strongly attractive, showing a resonance-like behavior. In the Nijmegen model-F, the hard-core radius of the  $YN$  potential is determined for each  $SU_3$  representation of the two-baryon configurations. Since the  $SU_3$  content of the  $\Sigma N(I = 3/2) {}^1P$  system is (30) and has no direct connection to any other  $NN$ ,  $\Lambda N$  and  $\Sigma N$  channels, the hard core radius of this channel is not well determined. The Nijmegen group determined the radius by fitting the low-energy  $\Sigma^+p$  scattering differential cross sections of large error bars. We will show in a separate paper<sup>22)</sup> that our phase shifts reproduce the low-energy  $\Sigma^+p$  cross sections equally well, but do not give a big rise in the cross sections around  $p_{\Sigma} \sim 450$  MeV/ $c$  unlike the Nijmegen hard-core models. The  $\Sigma^+p$  experiments will be very useful in this respect.

Figure 4 exhibits the equivalent local potentials for the  $NN$  and  $YN {}^1S$  channels at two incident momenta  $p_{lab} = 200$  and 600 MeV/ $c$ . The potential depth at 1 fm and at

$p_{lab} = 200$  MeV/ $c$  is  $-61$ ,  $-45$ , and  $-33$  MeV for the  $NN$ ,  $\Sigma N(I = 3/2)$ , and  $\Lambda N$  systems, respectively. It decreases when the energy increases. The core height at the origin is fairly low.

## VI. SUMMARY

A resonating-group (RGM) formulation of the  $(3q)$ - $(3q)$  system in the  $SU_6$  quark model is presented to study the central part of the hyperon-nucleon ( $YN$ ) interaction. The quark-quark interaction taken from the Fermi-Breit interaction includes the color-Coulombic term, the momentum-dependent retardation term and the color-magnetic contact term. The confinement potential put in by hand plays no active role in producing the  $YN$  interaction. Since the physics of  $YN$  properties is basically the study of the flavor symmetry breaking (FSB), it is important to use such a formalism that makes the consequence of the breaking as transparent as possible. For this purpose we have extensively used the spin-flavor  $SU_6$  symmetries of the  $YN$  systems. Assuming that the spatial part of the octet baryon is flavor independent, we have introduced the FSB through the mass difference of the strange and up-down quarks and the mass difference among the octet baryons: The former appears through the mass term of the Fermi-Breit interaction, while the latter gives substantial effects on the phase-shift behavior via the reduced mass of the  $YN$  relative motion.

We have pointed out that the basic features of  $S$ - and  $P$ -wave  $YN$  interaction exemplified by the Nijmegen models can be best understood in the classification of the spin-flavor symmetry of the  $YN$  system. It is possible not only to clarify the close relationship between the quark Pauli effect and the phase-shift patterns, but also to correlate the qualitative nature of the interaction strength among the  $YN$  systems. This important result has been demonstrated by solving the RGM equation with the quark-quark interaction turned off. This analysis is further extended to show two characteristic properties of the medium-range central attraction which is missing in the  $(3q)$ - $(3q)$  quark model: One is that the needed attraction must be stronger in the flavor symmetric channels than in the antisymmetric

channels. The other is that the needed attraction must have proper dependence on the  $YN$  channels, because otherwise one cannot reproduce the splitting of the phase shifts of the  $YN$  systems. We stress that this conclusion can be reached only when proper care is taken of the reduced mass of the  $YN$  system. Since the momentum-dependent retardation term gives a large contribution to the reduced mass, it is important to calculate the direct and the exchange terms of this piece of interaction exactly in the total center-of-mass system. The exchange kernel is then renormalized such that the whole momentum-dependence from the direct terms takes the form of the standard non-relativistic kinetic-energy term with the correct empirical reduced mass. This procedure utilizes the advantages of the RGM framework that a particular contribution of the quark-model Hamiltonian can be isolated in the analytic form and enables us to temper rather drastic effect of the relativistic correction in the present non-relativistic framework.

The flavor-dependent medium-range effective attraction has been conveniently constructed from the scalar-meson nonet exchange potentials of the Nijmegen model-F. The spatial structure of the octet baryon is taken into account in constructing the effective attractive potentials through the form factor of the  $(3q)$  clusters. We have applied the WKB approximation to the RGM equation with this effective meson-exchange potentials to calculate the phase shifts and the phase-shift equivalent local potentials. Two parameters which determine the strength of the effective attraction are fixed to fit the  $NN$   $^1S$  and  $^3S$  phase shifts. With only these two parameters, various  $YN$  phase shifts have exhibited a nice correspondence with those given by the Nijmegen model-F. The resultant  $YN$  central potentials are found to be less attractive than the  $NN$  potential, which leads to the splitting of the  $NN$  and  $YN$  phase shifts. The FSB of the medium-range attraction dominantly originates from both the singlet-octet meson mixing and the mass difference in the scalar-meson nonet. An only noticeable disagreement is the  $\Sigma N(I = 3/2)$   $^1P$  phase shift: The Nijmegen hard-core model shows a resonance-like behavior at  $p_E \sim 450$  MeV/ $c$ , while our model gives rather moderate attractive phase shifts.

There remain a few problems for further studies. One is concerned with the fact that

the reduced mass is not correctly given in the RGM framework. The procedure given in the present paper can be applied to a single-channel case, but is not straightforwardly applicable to coupled-channel problems such as  $\Lambda N$  and  $\Sigma N(I = 1/2)$  systems. The second is that we have to go beyond the WKB-RGM formalism. This is obviously necessary since in some channels we do not have physical solutions of the transcendental equation. To avoid this situation, we have to solve the RGM equation directly for the systems in which the medium-range attraction emerges from some appropriate quark-quark interaction. As we have found in this paper, the medium-range attraction must have proper flavor dependence. It is not, however, apparent nor unique how such flavor dependence should be realized from the underlying quark-quark interaction. The third is that we have to calculate cross sections to have more complete understanding of the  $YN$  interaction. Obviously, we have to consider non-central parts of the interaction. As we have discussed in Ref.13), the spin-orbit force can be accounted for by the quark model. It is clear that the tensor component is not given sufficiently in the quark model. In the forthcoming papers,<sup>22)</sup> we plan to extend the present model by including the spin-spin central and tensor terms from the pseudo-scalar  $\pi$ - and  $K$ -meson exchanges.

#### ACKNOWLEDGMENTS

The authors would like to thank members of Nuclear Theory Groups of Niigata and Kyoto Universities for useful discussions. They also would like to acknowledge the generous grants of computer time by the Research Center for Nuclear Physics, Osaka University. This work was supported by Grant-in-Aid for Scientific Research (C) from the Ministry of Education, Science and Culture (04640296).



## REFERENCES

- [1] H. Bando, Y. Yamamoto, T. Motoba, K. Ikeda and T. Yamada, Prog. Theor. Phys. Suppl. No. 81 (1985), 1 ; H. Bando, T. Motoba and J. Žofka, Int. Mod. Phys. **A21** (1990), 4021 ; C. B. Dover and A. Gal, Prog. Part. Nucl. Phys. **12** (1984), 171.
- [2] M. M. Nagels, T. A. Rijken and J. J. de Swart, Phys. Rev. **D15** (1977), 2547.
- [3] M. M. Nagels, T. A. Rijken and J. J. de Swart, Phys. Rev. **D20** (1979), 1633.
- [4] B. Holzenkamp, K. Holinde and J. Speth, Nucl. Phys. **A500** (1989), 485.
- [5] A. Reuber, K. Holinde and J. Speth, Nucl. Phys. **A570** (1994), 543.
- [6] M. Oka and K. Yazaki, in *Quarks and Nuclei*, ed. W. Weise (World Scientific, Singapore, 1984), p.489 ; K. Shimizu, Rep. Prog. Phys. **52** (1989), 1 ; C.W. Wong, Phys. Rep. **136** (1986), 1.
- [7] S. Takeuchi, K. Shimizu and K. Yazaki, Nucl. Phys. **A504** (1989), 777.
- [8] Y. Fujiwara and K.T. Hecht, Nucl. Phys. **A444** (1985), 541 ; **A451** (1986), 625 ; **A456** (1986), 669 ; **A462** (1987), 621 ; K. T. Hecht and Y. Fujiwara, Nucl. Phys. **A463** (1987), 255c.
- [9] M. Oka, K. Shimizu and K. Yazaki, Nucl. Phys. **A464** (1987), 700.
- [10] U. Straub, Zhang Zong-Ye, K. Bräuer, Amand Faessler, S. B. Khadkikar and G. Lübeck, Nucl. Phys., **A483** (1988), 686 ; **A508** (1990), 385c.
- [11] Zong-ye Zhang, Amand Faessler, U. Straub and L. Ya. Glozman, Nucl. Phys., **A578** (1994), 573.
- [12] Y. Fujiwara, Prog. Theor. Phys. **90** (1993), 105.
- [13] C. Nakamoto, Y. Suzuki and Y. Fujiwara, Phys. Letters **B318** (1993), 587.
- [14] Y. Fujiwara, "RGM in Quark-Hadron Physics", *Soryushiron Kenkyu (Kyoto)* **87** (1993),

B147.

- [15] Y. Fujiwara, Prog. Theor. Phys. Suppl. No. 91 (1987), 160.
- [16] H. Horiuchi, Prog. Theor. Phys. **64** (1980), 184 ; K. Aoki and H. Horiuchi, Prog. Theor. Phys. **68** (1982), 1658 ; 2028.
- [17] Y. Suzuki and K. T. Hecht, Phys. Rev. **C27** (1983), 299 ; Nucl. Phys. **A420** (1984), 525 and **A446** (1985), 749 ; Y. Suzuki, Nucl. Phys. **A430** (1984), 539.
- [18] Y. Fujiwara, Prog. Theor. Phys. **88** (1992), 933.
- [19] Y. Suzuki, Prog. Theor. Phys. **50** (1973), 1302 ; H. Horiuchi, Prog. Theor. Phys. Suppl. No. 62 (1977), 90.
- [20] K. Yazaki, Prog. Theor. Phys. Suppl. No. 91 (1987), 146.
- [21] S. Saito, Prog. Theor. Phys. **40** (1968), 893 ; **41** (1969), 705.
- [22] Y. Fujiwara, C. Nakamoto and Y. Suzuki, under preparation.

Table I. The  $SU_3$  content of the isospin basis  $B_1B_2$  with the definite flavor symmetry  $\mathcal{P}$ . See Eq.(2.5). The  $SU_3$  label  $(\lambda\mu)$  or  $(11)_\rho$  denotes the  $SU_3$ -coupled basis in Eq.(2.1).

$I$	$\mathcal{P} = +1$ (symmetric)	$\mathcal{P} = -1$ (antisymmetric)
	${}^1E$ or ${}^3O$	${}^3E$ or ${}^1O$
0	—	$NN = (03)$
1	$NN = (22)$	—
1/2	$\Lambda N = \frac{1}{\sqrt{10}}[(11)_s + 3(22)]$	$\Lambda N = \frac{1}{\sqrt{2}}[-(11)_a + (03)]$
1/2	$\Sigma N = \frac{1}{\sqrt{10}}[3(11)_s - (22)]$	$\Sigma N = \frac{1}{\sqrt{2}}[(11)_a + (03)]$
3/2	$\Sigma N = (22)$	$\Sigma N = (30)$

Table II. The  $S$ -wave and  $P$ -wave phase-shift behavior of the Nijmegen model-F central potentials classified by the flavor exchange symmetry  $\mathcal{P}$  and by the spin-orbital quantum numbers  ${}^{2S+1}L$ . The spin-flavor-color factors,  $X_N$ , of the exchange normalization kernel are also shown for comparison.

$B_1B_2$	$I$	$\mathcal{P} = +1$				$\mathcal{P} = -1$			
		${}^1S$		${}^3P$		${}^3S$		${}^1P$	
		phase shift	$X_N$	phase shift	$X_N$	phase shift	$X_N$	phase shift	$X_N$
$NN$	0	—	—	—	—	$< 19^\circ$	$\frac{1}{9}$	strong repulsion	$-\frac{7}{3}$
$NN$	1	$\leq 60^\circ$	$\frac{1}{9}$	weak repulsion	$-\frac{31}{27}$	—	—	—	—
$\Lambda N$	$\frac{1}{2}$	$< 23^\circ$	0	weak repulsion	-1	$< 6^\circ$	0	weak repulsion	-1
$\Sigma N$	$\frac{1}{2}$	strong repulsion	$-\frac{8}{9}$	$< 9^\circ$	$\frac{5}{27}$	$< 4^\circ$	0	weak repulsion	-1
$\Sigma N$	$\frac{3}{2}$	$< 36^\circ$	$\frac{1}{9}$	weak repulsion	$-\frac{31}{27}$	strong repulsion	$-\frac{7}{9}$	$\leq 70^\circ$	$\frac{1}{3}$

Table III. The  $S$ -wave phase shifts calculated in the Saito model for channels with three different  $X_N$  values. The symbol  $\tilde{K}$  stands for the calculation including only the kinetic energy term, and  $\tilde{K} + \tilde{MC}$  both of the kinetic-energy and  $U^{MC}$  terms. The parameter  $\lambda$  denotes the ratio of the strange to up-down quark mass  $m_s/m_{ud}$ . The ratio  $\zeta = \mu_\alpha/\mu_\alpha^{exp}$  in Eq. (4.1) or (4.2) is also shown.

$p_{lab}$ (MeV/c)	$X_N = \frac{1}{9}$				$X_N = 0$	
	$NN {}^1S$		$\Sigma N(\frac{3}{2}) {}^1S$		$\Lambda N {}^1S$	$\Sigma N(\frac{1}{2}) {}^3S$
	$\tilde{K}$	$\tilde{K} + \tilde{MC}$	$\tilde{K} + \tilde{MC}$		$\tilde{K} + \tilde{MC}$	$\tilde{K} + \tilde{MC}$
	—	—	$\lambda = 1$	$\lambda = 1.69$	$\lambda = 1.69$	$\lambda = 1.69$
	$\zeta = 1.000$	$\zeta = 0.4691$	$\zeta = 0.4192$	$\zeta = 0.4679$	$\zeta = 0.4822$	$\zeta = 0.4679$
200	10.49	8.18	7.52	9.61	-4.45	0.91
400	12.15	9.98	10.09	12.23	-6.16	1.19
600	8.78	7.54	8.60	9.93	-4.63	0.88
800	4.62	4.12	5.59	6.17	-2.05	0.42
1000	1.39	1.24	2.62	2.79	-0.51	0.12

$p_{lab}$ (MeV/c)	$X_N = -\frac{8}{9}$		
	$\Sigma N(\frac{1}{2}) {}^1S$		
	$\tilde{K}$	$\tilde{K} + \tilde{MC}$	
	$\lambda = 1$	$\lambda = 1$	$\lambda = 1.69$
	$\zeta = 0.8935$	$\zeta = 0.4192$	$\zeta = 0.4679$
200	-24.10	-22.38	-23.03
400	-46.90	-43.45	-44.72
600	-67.19	-62.02	-63.86
800	-83.70	-76.78	-79.11
1000	-92.81	-83.84	-86.59

Figure Caption

Figure 1. The  $S$ - and  $P$ -wave phase shifts calculated with the central potentials of Nijmegen model-F. The coupling potential between  $\Lambda N$  and  $\Sigma N(I = 1/2)$  channels is turned off.

Figure 2. The  $S$ - and  $P$ -wave phase shifts calculated in the Saito model. The momentum-dependent retardation term  $U^{MC}$  is turned off. The value of  $\lambda$  is set equal to unity. The round brackets imply small difference of the phase shifts originating from the baryon masses used in the c.m.-lab. transformation of the incident momentum.

Figure 3. The comparison of the phase shifts between the present model and Nijmegen model-F. Closed circle( $\bullet$ ), cross( $\times$ ), square( $\square$ ) and diamond( $\blacklozenge$ ) denote  $NN$ ,  $\Lambda N$ ,  $\Sigma N(I = 3/2)$  and  $\Sigma N(I = 1/2)$  phase shifts of Nijmegen model-F, respectively.

Figure 4. The equivalent local potentials of the  $^1S$  channel at  $p_{lab} = 200$  and  $600$  MeV/c. Solid, dashed and dash-dotted curves correspond to  $NN$ ,  $\Lambda N$  and  $\Sigma N(I = 3/2)$  cases, respectively.

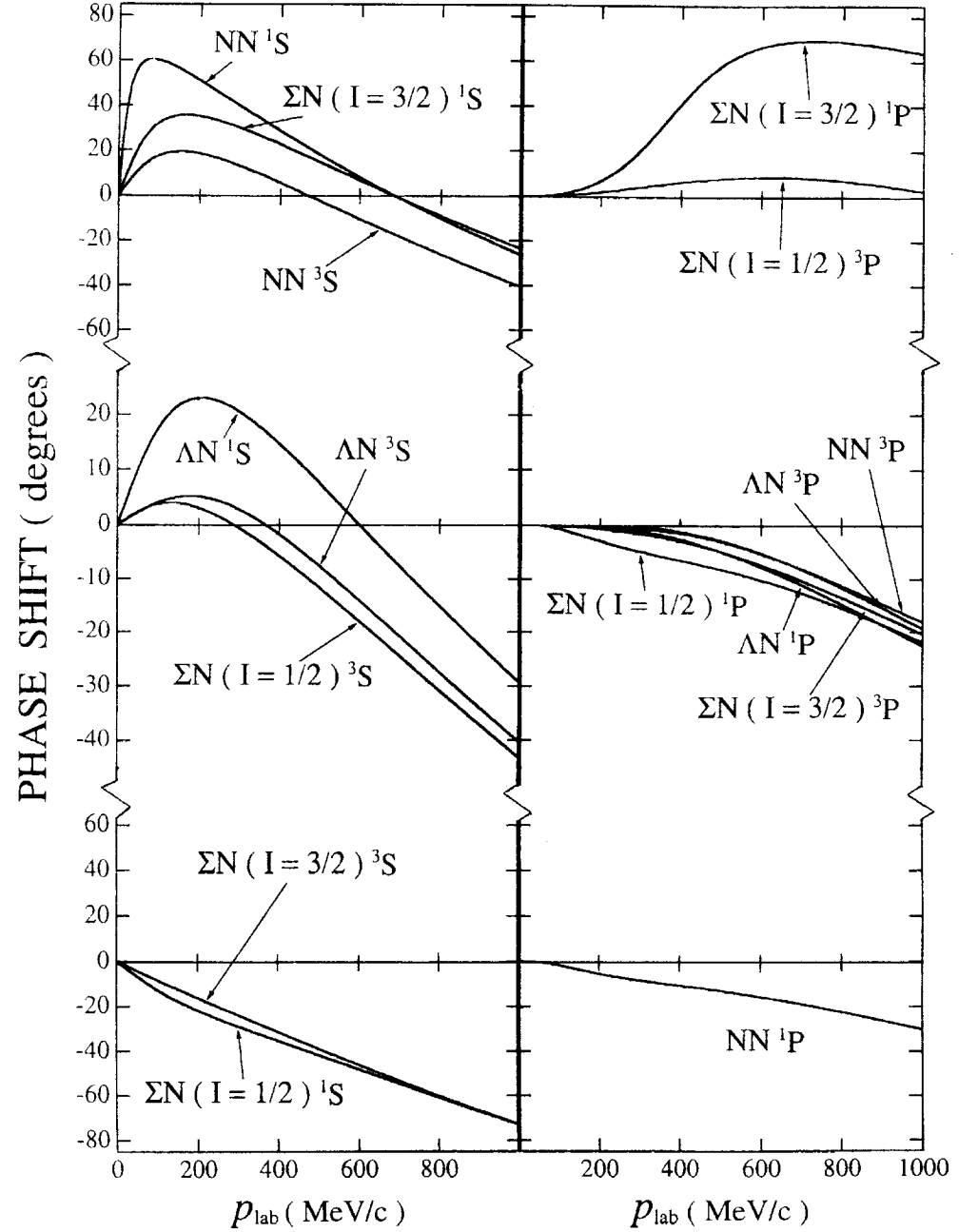


Fig.1

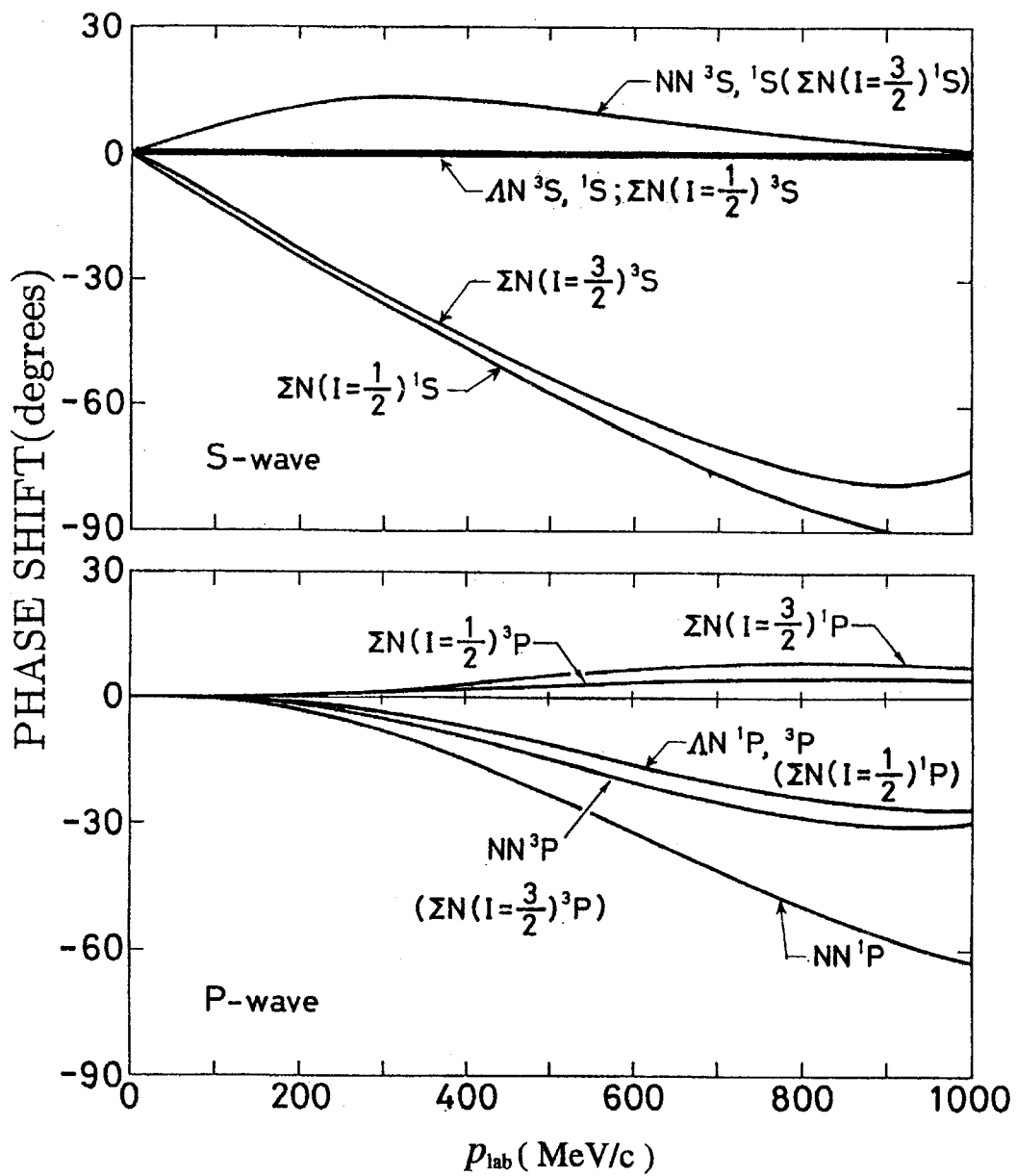


Fig.2

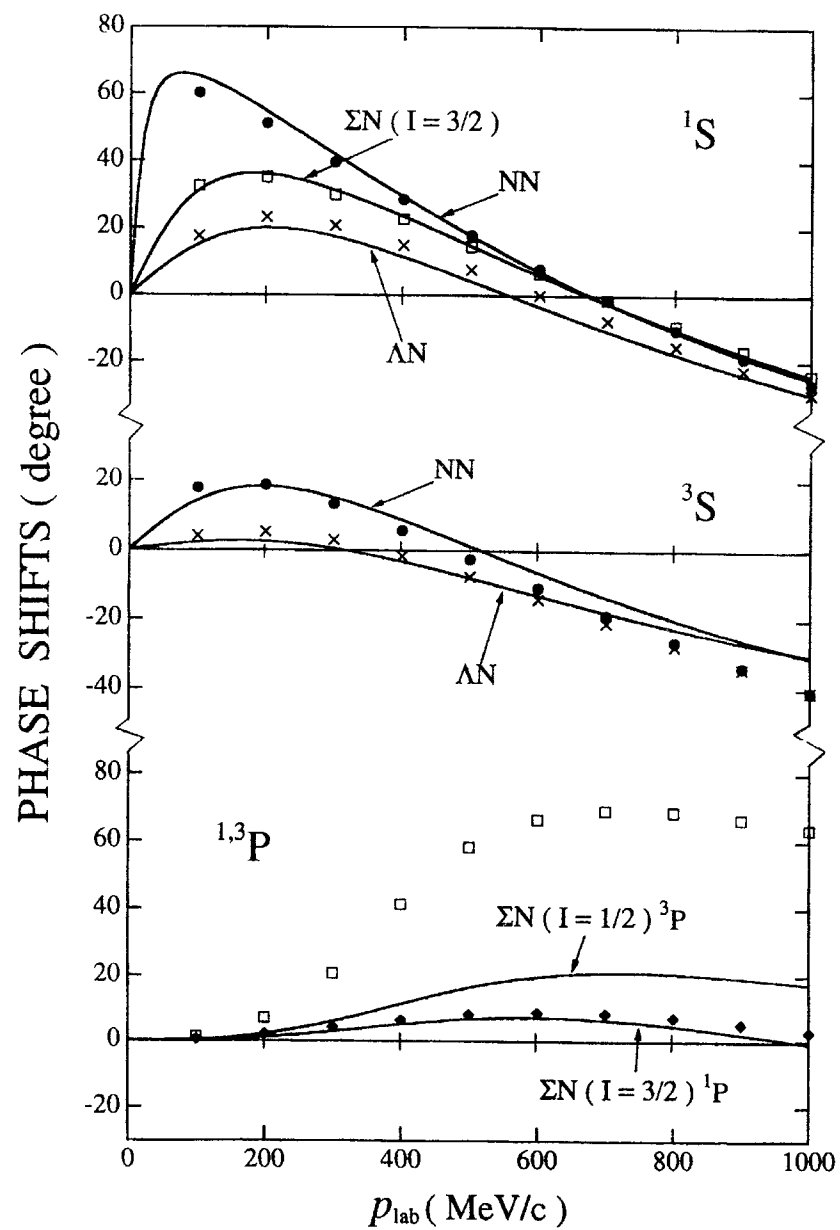


Fig.3

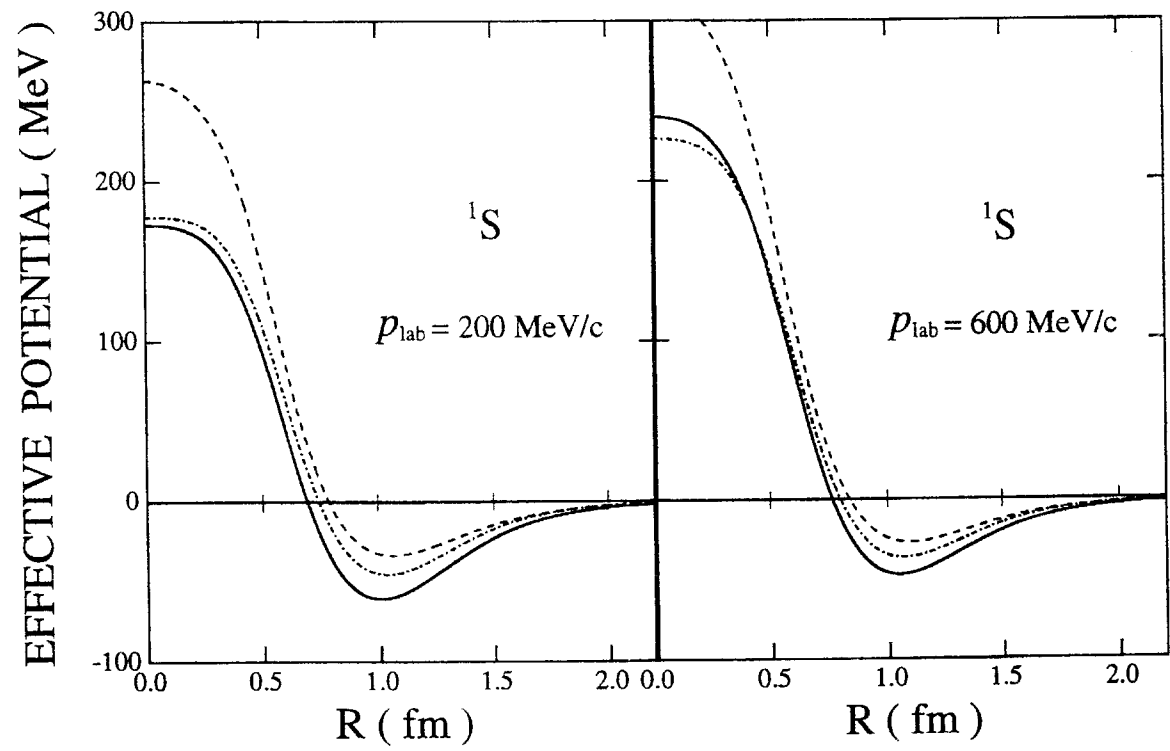


Fig.4

